



## A Multimethod Approach for Investigating Algal Toxicity of Platinum Nanoparticles

Sørensen, Sara Nørgaard; Engelbrekt, Christian; Lützhøft, Hans-Christian Holten; Jiménez-Lamana, Javier; Noori, Jafar Safaa; Al Atraktchi, Fatima Al-Zahraa; Giron Delgado, Cristina; Slaveykova, Vera I.; Baun, Anders

*Published in:*  
Environmental Science and Technology

*Link to article, DOI:*  
[10.1021/acs.est.6b01072](https://doi.org/10.1021/acs.est.6b01072)

*Publication date:*  
2016

*Document Version*  
Peer reviewed version

[Link back to DTU Orbit](#)

*Citation (APA):*  
Sørensen, S. N., Engelbrekt, C., Lützhøft, H-C. H., Jiménez-Lamana, J., Noori, J. S., Al Atraktchi, F. A-Z., Giron Delgado, C., Slaveykova, V. I., & Baun, A. (2016). A Multimethod Approach for Investigating Algal Toxicity of Platinum Nanoparticles. *Environmental Science and Technology*, 50(19), 10635–10643.  
<https://doi.org/10.1021/acs.est.6b01072>

---

### General rights

Copyright and moral rights for the publications made accessible in the public portal are retained by the authors and/or other copyright owners and it is a condition of accessing publications that users recognise and abide by the legal requirements associated with these rights.

- Users may download and print one copy of any publication from the public portal for the purpose of private study or research.
- You may not further distribute the material or use it for any profit-making activity or commercial gain
- You may freely distribute the URL identifying the publication in the public portal

If you believe that this document breaches copyright please contact us providing details, and we will remove access to the work immediately and investigate your claim.

1 **TITLE**

2 A Multimethod Approach for Investigating Algal Toxicity of Platinum Nanoparticles

3

4 **AUTHORS AND AFFILIATIONS**

5 Sara N. Sørensen<sup>†\*</sup>, Christian Engelbrekt<sup>‡</sup>, Hans-Christian H. Lützhøft<sup>†</sup>, Javier Jiménez-Lamana<sup>§</sup>, Jafar

6 S. Noori<sup>||</sup>, Fatima A. Alatraktchi<sup>⊥</sup>, Cristina G. Delgado<sup>†</sup>, Vera I. Slaveykova<sup>§</sup> and Anders Baun<sup>†</sup>

7

8 <sup>†</sup>Department of Environmental Engineering, Technical University of Denmark, Kgs. Lyngby, Denmark

9 <sup>‡</sup>Department of Chemistry, Technical University of Denmark, Kgs. Lyngby, Denmark

10 <sup>||</sup>IPM-Intelligent Pollutant Monitoring, Copenhagen, Denmark

11 <sup>⊥</sup>Department of Micro- and Nanotechnology, Technical University of Denmark, Kgs. Lyngby,

12 Denmark

13 <sup>§</sup>Environmental Biogeochemistry and Ecotoxicology, Institute F.-A. Forel, Earth and Environmental

14 Sciences, Faculty of Sciences, University of Geneva, Geneva, Switzerland

15

16 **CORRESPONDING AUTHOR**

17 Name: Sara Nørgaard Sørensen

18 Address: Department of Environmental Engineering, Technical University of Denmark

19 Miljøvej, Building 113, DK-2800 Kgs. Lyngby, Denmark

20 Phone: +45 45251688 or +45 28556482

21 Fax: +45 45932850

22 E-mail: [sans@env.dtu.dk](mailto:sans@env.dtu.dk)

23

## ABSTRACT

24

25 The ecotoxicity of platinum nanoparticles (PtNPs) widely used in for example automotive catalytic  
26 converters, is largely unknown. This study employs various characterization techniques and toxicity  
27 endpoints to investigate PtNP toxicity towards the green microalgae *Pseudokirchneriella subcapitata*  
28 and *Chlamydomonas reinhardtii*. Growth rate inhibition occurred in standard ISO tests (EC<sub>50</sub> values of  
29 15-200 mg Pt/L), but also in a double-vial setup, separating cells from PtNPs, thus demonstrating  
30 shading as an important artefact for PtNP toxicity. Negligible membrane damage, but substantial  
31 oxidative stress was detected at 0.1-80 mg Pt/L in both algal species using flow cytometry. PtNPs  
32 caused growth rate inhibition and oxidative stress in *P. subcapitata*, beyond what was accounted for by  
33 dissolved Pt, indicating NP-specific toxicity of PtNPs. Overall, *P. subcapitata* was found to be more  
34 sensitive towards PtNPs and higher body burdens were measured in this species, possibly due to a  
35 favored binding of Pt to the polysaccharide-rich cell wall of this algal species. This study highlights the  
36 importance of using multi-method approaches in nanoecotoxicological studies to elucidate toxicity  
37 mechanisms, influence of NP-interactions with media/organisms, and ultimately to identify artefacts  
38 and appropriate endpoints for NP-ecotoxicity testing.

## INTRODUCTION

39

40 The aquatic fate and toxicity of various metal nanoparticles have been studied intensively in recent  
41 years,<sup>1</sup> but very few studies have focused on the effects of platinum nanoparticles (PtNPs) on aquatic  
42 organisms. This is somewhat surprising considering the extensive use of PtNPs in automotive catalytic  
43 converters during the past decades. In the three-way catalytic converter, Pt is wash-coated onto a  
44 ceramic carrier and deposited as NPs,<sup>2</sup> typically in the size range of 1-10 nm.<sup>3</sup> The well-known  
45 catalytic activity of Pt is improved for nanostructured particles, allowing for an increased specific  
46 surface area of the Pt.<sup>4</sup> During use, abrasion of the catalytic converter will cause emission of Pt to the  
47 environment, mainly as elemental nanocrystalline Pt attached to  $\mu\text{m}$ -sized alumina particles.<sup>5</sup>  
48 Automotive catalysts represent the largest use of Pt and one of the main sources for emissions into the  
49 environment.<sup>6</sup> Emitted particles will be spread in the environment via atmospheric transport and/or  
50 stormwater runoff into drainage systems. Thus, elevated Pt levels have been detected in roadside dust,  
51 river sediments, aquatic organisms<sup>6,7</sup> and even in Greenlandic snow isolated from heavy traffic.<sup>8</sup>  
52 The ecotoxicological effects of PtNPs in the aquatic environment remains, however, largely unknown.  
53 Zebrafish embryos exposed to 3-10 nm PtNPs capped with polyvinyl alcohol, showed hatching delays,  
54 concentration-dependent drop in heart rate, touch response, and axis curvature.<sup>9</sup> Similarly, 10 nm  
55 PtNPs influenced the heart rate of zebrafish embryos, as well as hatching and morphology, while also  
56 causing mortality and cytotoxicity in *in vitro* assays.<sup>10</sup> More recently, PtNPs in the size range of 30-60  
57 nm were shown to inhibit the growth of green algae with a 72 h mean effective concentration ( $\text{EC}_{50,72\text{h}}$ )  
58 of 17 mg Pt/L.<sup>11</sup>  
59 Algal toxicity data are required in hazard assessments schemes for chemical classification and  
60 regulation,<sup>12</sup> but NPs comprise a challenge to aquatic toxicity testing, due to their heterogeneous and  
61 dynamic nature when suspended in aqueous media.<sup>13</sup> This results in varying exposure concentrations

62 during incubation which ultimately affect the test validity and reproducibility.<sup>14-16</sup> The issue of NP  
63 transformation during incubation is further magnified for algal growth inhibition tests, due to the  
64 exponential increase in algal cells as well as the presence of their exudates and metabolic products.<sup>17</sup>  
65 The presence of relatively high concentrations of NPs in algal growth inhibition tests may also restrict  
66 light from reaching the algae, thereby causing growth inhibition as a result of a physical shading effect  
67 and not as an effect of toxicity to the algae.<sup>14,15,18</sup>

68 When conducting algal toxicity testing for regulatory purposes, the tested substances, are considered  
69 hazardous to the aquatic environment when the mean effective concentration (EC<sub>50</sub>) is  $\leq 100$  mg/L in  
70 tests with either algae, crustaceans or fish.<sup>12</sup> Consequently, the algal testing setup needs to be valid  
71 even at relative high NP-concentrations, compared to relevant environmental exposure concentrations.  
72 The algal test was originally developed for soluble chemicals, for which a high concentration is only  
73 problematic in the case of poorly soluble or very colored substances.<sup>19</sup> As NPs are not soluble  
74 chemicals, but rather particles suspended in the test medium, it is important to investigate testing  
75 artefacts, such as shading, to evaluate the appropriateness of the currently used standard tests.<sup>20</sup>

76 Currently, the outcome of standard toxicity testing is applied in hazard identification and regulation of  
77 NPs, although the mechanisms behind the test outcome rarely are understood completely. A testing  
78 scheme involving various endpoints may contribute to a better understanding of potential NP-specific  
79 ecotoxicological effects and form a more solid foundation for NP regulation.

80 This study aims to investigate potential mechanisms involved in the growth rate inhibition caused by  
81 PtNPs in the standard algal test used for hazard identification purposes. A multi-method approach is  
82 applied to elucidate the role of: 1) Physical obstruction of light, referred to as shading, 2) Cellular  
83 effects including oxidative stress and membrane damage, 3) Dissolution of PtNPs, and 4) Association  
84 of PtNPs to algal cells, determined as measured body burdens. Different biological endpoints are

85 compared for PtNPs and dissolved Pt (PtCl<sub>4</sub>) in two algal species *P. subcapitata* and *C. reinhardtii* and

86 paralleled with the aggregation and dissolution behavior of PtNPs in the respective algal media.

87

## MATERIALS AND METHODS

88

### 89 **Test materials, chemical analysis and preparation of test suspensions**

90 The PtNPs were synthesized as described by Engelbrekt and co-workers,<sup>4</sup> yielding an aqueous  
91 suspension of pH~4, containing residual amounts of starch (0.6% weight in total), 6 mM glucose, 4  
92 mM gluconic acid, 10 mM 2-(N-morpholino)ethanesulfonic acid (MES), 9 mM K<sup>+</sup> and 12 mM Cl<sup>-</sup>. The  
93 starch stabilized PtNPs have a primary metal core diameter of  $1.7 \pm 0.2$  nm and an outer diameter  
94 (including the starch coating) of 5.8-6.0 nm as determined by transmission electron microscopy (TEM)  
95 and thermogravimetric analysis.<sup>4</sup> The nominal Pt concentration of 390 mg Pt/L in the synthesized  
96 suspension was confirmed by inductively coupled plasma – mass spectrometry (ICP-MS; Agilent 7700,  
97 Morges, Switzerland) upon *aqua regia* digestion, yielding an average recovery of  $109 \pm 1\%$  (n=3).  
98 The two algal species *P. subcapitata* and *C. reinhardtii* were cultivated in ISO 8692 medium,<sup>21</sup> and  
99 four-fold diluted Tris-Acetate-Phosphate medium,<sup>22</sup> respectively (referred to hereafter as ISO and  
100 TAP4 media). Prior to all characterization and algal toxicity testing, a stock suspension was prepared  
101 from an aliquot of the synthesized suspension by adjusting the pH using 1 M NaOH and adding algal  
102 nutrients to match the two algal test media. These stock suspensions were then diluted further with  
103 algal medium to prepare the test concentrations. The Pt concentration in selected stock and diluted test  
104 suspensions of both PtCl<sub>4</sub> (0.1-400 mg Pt/L) and PtNPs (10-390 mg Pt/L) was measured by ICP-MS  
105 upon preparation. PtNPs were digested before ICP-MS by evaporating the media and re-dissolving the  
106 solid fraction in *aqua regia*. The average recovery was  $85 \pm 15\%$  (n=66). A series of studies on abiotic  
107 ROS generation was carried out with a second batch of PtNP synthesized as outlined above. For this  
108 batch the average recovery was  $68 \pm 9.6\%$  (n=6) in media suspensions of 1-200 mg Pt/L. Platinum (IV)  
109 chloride (PtCl<sub>4</sub>, 96%) was purchased from Sigma-Aldrich and included as a soluble Pt material. Other

110 reagents were analytical grade and all suspensions were prepared with Ultrapure Milli-Q water (> 18.2  
111 Ω Milli-Q Direct system, Merck Millipore, Darmstadt, Germany).

112

### 113 **Characterization of PtNPs suspended in algal media**

114 The size distributions and zeta potentials of PtNPs in algal media were determined by Dynamic Light

115 Scattering (DLS) using a Malvern ZetaSizer Nano ZS (Malvern Instruments, Malvern, UK).

116 Measurements were conducted 1, 24 and 48 h after preparation of the PtNP suspensions of 30 mg Pt/L

117 in TAP4 and ISO medium, respectively. The size distributions of PtNPs suspended in both media were

118 also determined by Asymmetric Flow Field-Flow Fractionation (AsFIFFF) using an AF2000 (Postnova

119 Analytics, Landsberg, Germany) immediately upon preparation and after 1, 24 and 48 h. For the

120 elemental detection, the AsFIFFF system was coupled to an ICP-MS (Agilent 7700, Morges,

121 Switzerland) monitoring the <sup>195</sup>Pt signal. The outflow of the AsFIFFF system was connected directly to

122 the nebulizer of the ICP-MS.

123 The PtNP agglomeration and sedimentation behavior during 48 h in the two media were investigated

124 respectively by nanoparticle tracking analysis (NTA) with a NanoSight LM10 (Malvern Instrument,

125 Malvern, UK) and spectrophotometry (Agilent 8453, Agilent Technologies, USA). The PtNP

126 suspensions (80 mg Pt/L) were prepared as for toxicity testing, and stored at 4 °C between

127 measurements, with TAP4 and ISO media as blank references. The measurements were conducted 1,

128 24 and 48 h after preparation of suspensions. The size and number of agglomerates (> ≈ 50 nm) present

129 in the suspensions were determined using NTA 3.1 with automated settings, camera level 16 and a

130 detection threshold of 5. For each measurement, three videos of 60 s were recorded and the sample

131 advanced before each video. Sedimentation was investigated by recording the absorbance of

132 suspensions at wavelengths ranging from 190 to 1100 nm.

133 The concentration of dissolved Pt in the stock suspensions of PtNPs and dilutions in algal media was  
134 determined by ultracentrifugation (Beckman L8-60M) using a swinging bucket rotor (SW 41 Ti;  
135 Beckman). PtNPs were suspended at 68 mg Pt/L in Milli-Q, ISO and TAP4 media. Immediately upon  
136 suspension, and after 48 h incubation under algal testing conditions, samples of 10 mL (n=2) were  
137 centrifuged for 16 h at  $3 \times 10^4$  rpm ( $68000 \times g$ ) to ensure settling of particles  $\geq 5.7$  nm. The supernatant  
138 (5 mL) was removed, acidified with nitric acid and the Pt content was measured by ICP-MS.  
139 The abiotic generation of reactive oxygen species (ROS) by PtNPs and PtCl<sub>4</sub> suspended in algal media  
140 (without algae present) was determined using the fluorescent dye 2',7'-dichlorodihydrofluorescein  
141 diacetate (H<sub>2</sub>DCF-DA, Sigma Aldrich) as described by Ivask and co-workers.<sup>23</sup> Specific details are  
142 given the Supporting Information (SI).

143

#### 144 **Algal growth rate inhibition and <sup>14</sup>C-assimilation tests**

145 Tests were performed in accordance with the ISO 8692 algal growth inhibition test protocol<sup>21</sup> with  
146 modifications as described below, and 48 h incubation.<sup>24</sup> Tested concentrations (n=3) and controls  
147 (n=6) were inoculated with algae ( $10^4$  cells/mL) yielding average control growth rates of 1.0-1.3 d<sup>-1</sup> for  
148 *P. subcapitata* and 1.7-1.8 d<sup>-1</sup> for *C. reinhardtii*. A maximum pH change of 1.7 units occurred in  
149 controls as well as exposed algae during the 48 h incubation. The quantity of algal pigments was  
150 quantified at 0, 24 and 48 h by acetone extraction<sup>25</sup> followed by fluorescence spectrophotometry  
151 (Hitachi F-7000) at 430 and 670 nm excitation and emission wavelengths, respectively. The <sup>14</sup>C-  
152 incorporation was performed as described in previous work<sup>16</sup> (details are included in SI). A maximum  
153 change in pH of 1.5 units was measured during the 2 h incubation.

154 The influence of PtNPs' shading on algal growth rates and <sup>14</sup>C-assimilation inhibition was studied  
155 under the same conditions as described above, but using a double-vial test setup. Algae in media (2

156 mL) were kept in a small inner-vial, and physically separated from the PtNP suspension (6 mL) placed  
157 in the larger outer-vial (Figure S1). The control growth rates were in the range given for the regular  
158 setup. Finally, the potential photochemical efficiency was monitored over 48 h in algae exposed to 0, 2  
159 and 80 mg Pt/L, as described in the SI.

160

### 161 **Algal cell damage and oxidative stress**

162 Test suspensions were prepared in volumetric flasks, inoculated to  $10^5$  cells/mL and distributed (25  
163 mL, n=3) to 100 mL Erlenmeyer flasks incubated as described in the SI. Tests with PtCl<sub>4</sub> were  
164 conducted using the setup for growth inhibition tests. A maximum variation of 0.4 (PtNPs) and 1.3  
165 (PtCl<sub>4</sub>) pH-units was found before testing and after 48 h incubation in controls and the highest test  
166 concentrations. After 2, 24 and 48 h incubation, algae were sampled from each concentration and  
167 controls, and incubated with fluorescent dyes for 30 min in the dark. CellROX Green (Life  
168 Technologies Europe B.V., Zug, Switzerland) was employed as intracellular oxidative stress indicator  
169 (5 μM), and propidium iodide (Sigma-Aldrich, Buchs, Switzerland) was used to determine membrane  
170 permeability alteration (7 μM), as previously described in details for *C. reinhardtii*.<sup>26,27</sup> Unexposed  
171 algae were used as negative controls, whereas the positive controls prior to staining, were incubated  
172 with 10 mM H<sub>2</sub>O<sub>2</sub> (30 min in the dark) and in a 90°C water bath (10 min) for CellROX Green and  
173 propidium iodide, respectively. Flow cytometry was conducted using a BD Accuri C6 flow cytometer  
174 (BD Biosciences, San Jose, CA, USA) with an argon-ion excitation laser (488 nm) and FL1 green  
175 channel (530 ± 15 nm), FL2 orange channel (585 ± 20 nm) and FL3 red channel (670 ± 25 nm). For  
176 tests with PtCl<sub>4</sub>, results were analyzed using a BD FACSCanto II flow cytometer (BD Biosciences, San  
177 Jose, CA, USA). Gating strategies were applied to discriminate positively stained cells from the

178 negative control (Figure S2-4). Data analysis was conducted using BD Accuri C6 software 264.15 and  
179 FlowJo V10 for the two flow cytometers, respectively.

180

### 181 **Algal body burden of PtNPs**

182 Algae were exposed to PtNPs (2 and 80 mg Pt/L) in triplicate 250 mL flasks with 75 mL suspension  
183 inoculated to  $10^5$  cells/mL. A sample of 20 mL suspension from each replicate was taken after 2, 24 and  
184 48 h incubation and filtered through a 3.0  $\mu\text{m}$  nitrocellulose filter (Merck Millipore). The algal cells  
185 retained by the filter were gently washed with 20 mL medium before filters were digested in Teflon  
186 tubes (1 mL *aqua regia* at 90°C for 2 h). The Pt content was determined by ICP-MS analysis (Agilent  
187 7700, Morges, Switzerland) after dilution with 5% (v/v) HCl (Baker, instar grade). The cell number for  
188 each replicate suspension was determined after 0, 2, 24 and 48 h incubation on a Coulter Multisizer III  
189 particle counter (Beckman-Coulter, Switzerland). Suspensions of PtNPs in media (80 mg Pt/L) without  
190 algae were applied as background controls, and treated as described above. The particle counts and Pt  
191 content of digested filters were all background corrected using data from these controls.

192

### 193 **Atomic force microscopy imaging**

194 For atomic force microscopy (AFM) both algal species were exposed to PtNPs (10 mg Pt/L) under the  
195 same conditions as described for growth inhibition testing. After 48 h incubation, a drop of each  
196 suspension was placed on sliced silicon wafers and allowed to dry. To remove dry salt particles, the  
197 wafer pieces were carefully washed with distilled water and dried again with nitrogen gas. Atomic  
198 Force Microscope (AFM NX20, Park Systems) images were taken of the two samples using non-  
199 contact mode, an amplitude of  $1.67 \times 10^6$  nm and a scan rate of 1 Hz.

200

201 **Statistical analysis and data interpretation**

202 Mean effective concentrations ( $EC_{50}$ ) and corresponding 95% confidence intervals for the inhibition of  
203 algal growth rates and carbon assimilation were estimated using the statistical program LOG457, which  
204 applies the log-logistic model for nonlinear regression analysis of responses versus concentration,  
205 minimizing the sum of squares between calculated and measured inhibitions.<sup>28</sup> Nominal concentrations  
206 were used, as the average Pt recovery from ICP-MS analyses was  $84 \pm 15\%$  in selected stock and test  
207 suspensions of  $PtCl_4$  and PtNPs (n=72). Comparison of growth rate inhibition data is based on  $EC_{50}$ -  
208 values and their variability provided by corresponding 95% confidence intervals.

209

## RESULTS AND DISCUSSION

### Characterization of PtNPs in algal media

The size distributions of PtNPs suspended in algal media were determined after 1, 24 and 48 h by AsFIFFF (4 mg Pt/L), DLS (30 mg Pt/L) and NTA (80 mg Pt/L), see Figure 1. A size peak of 10 nm was identified by AsFIFFF and DLS. For NTA the size detection limit is higher than 10 nm, but NTA measurements contribute with information about agglomeration of PtNPs in algal media. As shown in Figure 1C, the number of PtNP agglomerates (> 50 nm) increased almost three orders of magnitude in the TAP4 medium, whereas PtNPs in the ISO medium remained within the same order of magnitude over the 48 h period. The agglomerates formed were in the size range of 50-400 nm for both media; this finding is supported by the DLS measurements, showing hydrodynamic diameters within this range at all times measured (Figure 1B). Moreover, the measured zeta potentials of PtNP suspensions (20-25 mg Pt/L) after 1 and 48 hours indicated higher stability of PtNPs in ISO ( $-28 \pm 0.3$  mV) than in TAP4 medium ( $-15 \pm 0.9$  mV). Besides the increasing agglomerate number, agglomerate sizes increased with time according to NTA (Figure 1C). Although the PtNPs agglomerated substantially, especially in the TAP4 medium, the UV-VIS absorbance did not change during the 48 h, indicating that the PtNPs remained suspended, and did not settle in the suspensions (Figure S5). The ICP-MS analyses of samples fractionated using AsFIFFF showed constant Pt recoveries in ISO medium over time (around 80% ), whereas recoveries in TAP4 decreased from 80% at 0 h to 62% and 63% at 24 and 48 h, respectively (Table S2). This decrease may be due to agglomeration, as larger agglomerates will not elute from the channel and hence not be detected by ICP-MS.

The concentration of dissolved Pt in PtNPs suspensions (total concentration 68 mg Pt/L) prepared in Milli-Q water, ISO and TAP4 media and incubated for 48 h under algal testing conditions were in the ranges of 2.3-2.4 mg Pt/L (Milli-Q water suspensions), 2.0-2.2 mg Pt/L (ISO medium suspension) and

233 2.0-2.5 mg Pt/L (TAP4 medium suspension). The concentrations increased only slightly during the 48  
234 h incubation. This shows that dissolved Pt (corresponding to about 3% of the total Pt content) in the  
235 test suspensions mainly was non-reacted Pt from the particle synthesis.

236 For the abiotic ROS generation analyses of PtNPs and PtCl<sub>4</sub> in both algal media (Figure S6) a relatively  
237 high, and varying, background DCF fluorescence was measured. As a consequence, the abiotic ROS  
238 was determined concomitantly for both PtNPs and PtCl<sub>4</sub> in the two media within one test run, to allow  
239 for a relative comparison between the ROS generation of the two forms of Pt. It should be noted that  
240 these analyses were made using another batch of PtNPs than otherwise used in this study. The PtNPs in  
241 this new batch were synthesized as described in the Materials and Methods and identical primary  
242 diameters were obtained. The algal-free assay measuring abiotic ROS generation revealed increasing  
243 DCF fluorescence relative to the backgrounds in a concentration-dependent manner for PtNPs in both  
244 media. A slightly higher response was detected in the ISO medium compared to TAP4, especially after  
245 48 h. Conversely for PtCl<sub>4</sub>, the relative DCF fluorescence was greater in TAP4 than in ISO medium.

246 Collectively, these data suggest that abiotic ROS generation is influenced by the media and that abiotic  
247 ROS measured in the PtNP suspension cannot be solely ascribed to dissolved Pt. The abiotic ROS  
248 generation activity by PtNPs of various shapes has been reported as low, based also on a cell-free DCF  
249 assay.<sup>29</sup> Comparison of results is however challenged by differences in methods and media applied.

250

### 251 **Effects of PtNPs on algal photosynthesis, carbon assimilation and growth rate**

252 Exposure to PtNPs resulted in decreased growth rates of both *P. subcapitata* and *C. reinhardtii* in  
253 standard ISO tests, with EC<sub>50,48h</sub> values (95% confidence intervals in brackets) of 15 [13-16] and 201  
254 [173-235] mg Pt/L, respectively. Based on the results from tests with *P. subcapitata*, the PtNPs would  
255 be classified as “harmful” to algae in accordance with the CLP regulation.<sup>12</sup> These results are generally

256 in agreement with the reported  $EC_{50,72h}$  value of 17 mg Pt/L for growth inhibition in *P. subcapitata*  
257 exposed to PtNPs.<sup>11</sup> Due to the dark color of the suspensions, we hypothesized that PtNPs limited the  
258 available light for algal growth causing shading, thus inhibiting growth physically rather than by a toxic  
259 action of the PtNPs to the algal cells. As growth rate inhibition also occurred in the double-vial setup  
260 with no contact between algae and PtNPs, we cannot falsify this hypothesis. The growth rate inhibition  
261 found using the double-vial setup was however slightly lower than in the standard test setup with  
262  $EC_{50,48h} = 45 [30-68]$  and  $373 [167-838]$  mg Pt/L for *P. subcapitata* and *C. reinhardtii*, respectively  
263 (Figure 2A, C). These results suggest that physical shading from PtNPs lowered the algal growth rates,  
264 but also indicate that PtNPs inhibit algal growth rates by other means than shading, possibly by direct  
265 toxic effects. However, the higher response in the regular setup could also arise from PtNPs adhesion to  
266 the algal surface, potentially causing “localized” shading and/or interference with the membrane,  
267 nutrient uptake and other cellular processes involving the cell surface.<sup>14</sup> As described by Hjorth and co-  
268 workers<sup>30</sup>: “Shading and toxicity are not additive effects. The impact of shading cannot be eliminated  
269 by simply subtracting the effect observed in the shading test from the actual test. Deducting the effect  
270 of shading is more complicated for NPs as the exact mode of action is unknown and the observed  
271 effects are potentially multicausal.” Also, shading can mask or limit potential toxicity, because slowly  
272 growing algae under low light intensity are less sensitive to toxicants than faster growing algae.<sup>30</sup>  
273 In agreement with our results, shading effects have been reported to markedly influence growth rate  
274 inhibition in green algae exposed to gold NPs<sup>31</sup> and carbon nanotubes,<sup>32</sup> while studies with ZnO, CuO  
275 and TiO<sub>2</sub> have found shading negligible.<sup>14,33</sup> It is likely that exposure concentration, suspension color,  
276 and NP adhesion to algal surfaces are influencing factors on shading. Consequently, growth rate  
277 inhibition alone is not an appropriate endpoint for disclosing PtNP toxicity, as it does not allow for  
278 discrimination between direct toxic effects and indirect physical effects. For this reason, <sup>14</sup>C-

279 assimilation was included as an alternative endpoint to quantify the toxicity of PtNPs towards the two  
280 algal species (Figure 2B, D). Comparable EC<sub>50</sub> values were obtained for *P. subcapitata* and *C.*  
281 *reinhardtii* of 47 [43-50] and 37 [31-46] mg Pt/L, respectively, in the regular setup, and 32 [16-65] and  
282 32 [18-56] mg Pt/L in the double-vial setup. The slopes of the concentration response curves are  
283 however different between data from the shading and the regular test with *C. reinhardtii* (Figure 2B).  
284 As the EC<sub>50</sub> values does not differ between the regular and the double-vial setup, the 2 h <sup>14</sup>C-  
285 assimilation inhibition in both algal species may be solely ascribed to physical shading effects of  
286 PtNPs. Thus, the endpoint of 2 h carbon assimilation is even more sensitive to shading and/or less  
287 applicable for testing PtNP toxicity than the standard 48 h growth rate inhibition test.  
288 Using the ultracentrifugation results, concentration–response data for PtNPs were recalculated based on  
289 the dissolved Pt concentration rather than the total nominal concentration (Figure 2A, C). For *C.*  
290 *reinhardtii* these data aligned closely with the PtCl<sub>4</sub> data, as also seen by the overlapping 95%  
291 confidence intervals of the EC<sub>50</sub> values. Thus, the PtNP toxicity to this algal species may be caused by  
292 the dissolved Pt. For *P. subcapitata* however, data based on dissolved Pt showed greater inhibition than  
293 PtCl<sub>4</sub>, suggesting a possible NP-specific effect.  
294 Taken together, the 48 h growth inhibition data (Figure 2A, C) demonstrate that *P. subcapitata* is more  
295 sensitive to the toxic effects of both PtCl<sub>4</sub> and PtNPs than *C. reinhardtii*. Furthermore, the results from  
296 the double-vial setups indicate that *P. subcapitata* is more affected by shading than *C. reinhardtii*. It  
297 may be, that *P. subcapitata* is less efficient in adapting to light conditions over time, and thus more  
298 affected by this physical effect than *C. reinhardtii*. The potential photochemical efficiency monitored  
299 over 48 h in algae exposed to 0, 2 and 80 mg Pt/L (Figure S7 was indeed slightly lower for *P.*  
300 *subcapitata* than *C. reinhardtii*, both for controls and exposed algae. This agrees with the difference in

301 growth rate measured for the two algal species controls in growth rate inhibition tests (app. 1.1 vs. 1.8  
302  $d^{-1}$  for *P. subcapitata* and *C. reinhardtii*, respectively).

303 Overall, the results demonstrate that shading from PtNPs does occur and affects the growth rates  
304 measured in a standard guideline test. If the double-vial setup had not been applied, comparing the  
305 results for PtCl<sub>4</sub> and PtNPs in Figure 2 could easily be misinterpreted and lead to faulty conclusions.  
306 Due to the influence of shading, neither growth rate inhibition nor <sup>14</sup>C-assimilation can be considered  
307 appropriate endpoints to test algal toxicity of PtNPs for hazard identification purposes. As the PtNP  
308 toxicity may be attributed to dissolved Pt for *C. reinhardtii*, but not entirely for *P. subcapitata*, the NP-  
309 specific effect(s) found could be algal species specific though the behavior of PtNPs in the two  
310 different algal media used, may also affects the toxicity.

311

### 312 **Cellular effects of PtNPs in algae: Oxidative stress and membrane damage**

313 Extensive oxidative stress was observed for both algal species upon PtNP exposure, as demonstrated by  
314 the increasing percentage of stained cells (Figure 3A, B). *C. reinhardtii* was highly stressed after 2 h  
315 exposure to PtNPs, even at the lowest exposure concentration (0.1 mg Pt/L). However, the algal  
316 population recovered over time for all PtNP-concentrations up to 10 mg Pt/L. Some indication of  
317 recovery over time was also seen for *P. subcapitata*, although much less pronounced than for *C.*  
318 *reinhardtii*. After exposure to PtCl<sub>4</sub>, oxidative stress was only detected in *C. reinhardtii* with no  
319 indication of recovery over time as it was seen after exposure to PtNPs (Figure 3D). Interestingly, no  
320 signs of oxidative stress were detected in *P. subcapitata* upon PtCl<sub>4</sub> exposure (Figure 3C), indicating  
321 the oxidative stress from PtNP exposure is not related to the dissolved Pt. Despite the substantial  
322 percentage of cells with oxidative stress caused by PtNPs, the percentage of cells with membrane  
323 damage were < 2% for *P. subcapitata* and < 22% for *C. reinhardtii* (supporting data, Figure S8). This

324 suggests that the antioxidant systems of both algal species were able to cope with the oxidative stress  
325 induced by PtNPs, thereby preventing its progression to membrane damage. In vitro studies using  
326 human cell lines similarly report that PtNPs do not affect the membrane integrity.<sup>10,34,35</sup> Whether or not  
327 PtNPs induce oxidative stress in human cells is more ambiguous, with biotic ROS and oxidative stress  
328 from PtNPs being both confirmed<sup>36</sup> and rejected,<sup>29,35</sup> and even detoxification of ROS has been  
329 suggested.<sup>34</sup>

330

### 331 **Algal body burden of PtNPs**

332 Although exposed to similar PtNP concentrations in suspension, the Pt body burden differed greatly for  
333 the two algal species (Figure 4A, B). In general, the body burdens were higher for *P. subcapitata*,  
334 especially at the highest tested concentration of 80 mg Pt/L. This may explain the more pronounced  
335 h growth rate inhibition found for this algal species since higher attachment of PtNPs to the algal  
336 surface is likely to cause a higher (local) shading effect and/or toxicity. For *C. reinhardtii* the body  
337 burden decreased significantly over 48 h for 2 mg Pt/L, but increased slightly at 80 mg Pt/L. This  
338 observation correlates well with the oxidative stress pattern showing recovery at 2 mg Pt/L, but not at  
339 80 mg Pt/L (Figure 3). Conversely, *P. subcapitata* recovered slightly from oxidative stress after 48 h at  
340 the highest concentration of 80 mg Pt/L and the body burden also decreased with time at this  
341 concentration (Figure 3 and 4A). The differences in body burdens in the two algal species may relate to  
342 the different composition of their cell walls. The cell wall of *P. subcapitata* contains cellulose and  
343 polysaccharides, whereas the cell wall of *C. reinhardtii* does not,<sup>37</sup> but rather consists of several layers  
344 of glycoproteins.<sup>22</sup> It has been proposed, that while Pt (II) has higher affinity for amino acids and  
345 proteins, Pt (IV) may preferentially bind to a polysaccharide matrix.<sup>38</sup> This may explain why higher  
346 growth rate inhibition was found for *P. subcapitata* than *C. reinhardtii* upon PtCl<sub>4</sub>, and PtNP exposure.

347 Another factor influencing the body burden is the higher growth rate of *C. reinhardtii* compared to *P.*  
348 *subcapitata*. This causes the ratio of PtNPs to algal cells to decrease faster in *C. reinhardtii*, and thus  
349 yield a lower body burden after 48 h exposure to PtNPs.

350 In a separate series of tests, the two algal species were examined by AFM after 48 h exposure to PtNP,  
351 providing some indication of PtNP-agglomerates on the algal cell surface (Figure S9). Several studies  
352 have demonstrated how various NPs attach to the surface of algae.<sup>14,15,33</sup> Attachment of NPs to algae is  
353 most likely a dynamic process, changing the NP body burden over time depending on algal physiology  
354 and NP properties. This is an area that needs more investigation and could prove very useful for the  
355 interpretation of data from aquatic toxicity testing of NPs.

356

#### 357 **PtNP behavior in test media and related biological effects**

358 Overall, the characterization of PtNPs in algal media showed a higher degree of agglomeration and  
359 dissolution of PtNPs in the TAP4 medium, whereas slightly more abiotic ROS was generated in the  
360 ISO medium. The implications of these findings are discussed below, along with the possible  
361 connection between the toxicity endpoints, and the difference in toxicity of PtNPs vs. dissolved Pt.  
362 According to NTA, a significantly higher number of agglomerates was formed during 48 h incubation  
363 in the TAP4 medium (*C. reinhardtii*) than in the ISO medium (*P. subcapitata*). The lower PtNP body  
364 burden in *C. reinhardtii* cells may be linked to the agglomeration behavior in the TAP4 medium, as  
365 smaller particle sizes theoretically favor greater adhesion to the algal surface, due to the increased  
366 number of particles available for contact with the algae. The lower Pt body burden in *C. reinhardtii*  
367 may in turn explain why this species was less affected in the growth inhibition test with PtNPs, as less  
368 contact between algal cells and PtNPs also reduces any localized shading and/or physical effects.

369

370 Both AsFFFF and ultracentrifugation data showed higher dissolution of PtNPs in the TAP4 medium  
371 (*C. reinhardtii*) than in the ISO medium (*P. subcapitata*). The growth rate inhibition of *C. reinhardtii*  
372 could be explained by the dissolved fraction of Pt in the medium. For *P. subcapitata* however, the  
373 PtNPs caused higher growth rate inhibition than explained by the measured dissolved Pt. Furthermore,  
374 the oxidative stress responses in the two algal species were not governed by dissolved Pt. For *P.*  
375 *subcapitata* all cells were affected by PtNPs, but none by PtCl<sub>4</sub> (Figure 3). *C. reinhardtii* cells were  
376 affected by both PtNPs and PtCl<sub>4</sub>, but the presence of dissolved Pt cannot fully account for the level of  
377 oxidative stress nor the recovery observed when cells were exposed to PtNPs (Figure 3). To fully  
378 understand the role of dissolved Pt in algal toxicity, knowledge on speciation and binding to media  
379 components is crucial. Unfortunately, speciation data such as solubility constants is limited<sup>39</sup> and not  
380 included in speciation models such as MINTEQ. The main differences between the two media are the  
381 pH, buffer types and the content of chloride and organic components. The ISO medium (pH 8) contains  
382 sodium bicarbonate buffer, whereas TAP4 (pH 7) contains TRIS, sodium acetate and roughly half the  
383 chloride amount of the ISO medium. The speciation and solubility of Pt is influenced by chloride  
384 species, pH, and organic ligands such as citric acid.<sup>39-41</sup> However, determining the exact Pt speciation  
385 in the actual media is challenged by the different scopes and variables of available speciation studies,  
386 as well as the obscure number of chemical species found even in a simple system of Pt, chloride and  
387 water.<sup>41</sup>

388 Abiotic ROS, generated by PtNPs when suspended in the two algal media, may have caused or  
389 contributed to the oxidative stress detected in both algal species. Abiotic ROS was however, also  
390 generated by PtNPs in Milli-Q water (data not shown) suggesting that the ROS generation from PtNPs  
391 may occur on the surface of PtNPs. This is further supported by the results of the positive controls in  
392 the tests of abiotic ROS (Figure S6) and oxidative stress (Figure S3 and S4) as no abiotic ROS or

393 oxidative stress occurred from the positive control (H<sub>2</sub>O<sub>2</sub>) or the dissolved reference (PtCl<sub>4</sub>) in the ISO  
394 medium, whereas PtNPs caused very clear responses in both these tests. Similarly, it has been  
395 suggested by other publications that NPs may induce elevated intracellular ROS by direct  
396 physical/chemical interactions with biomolecules.<sup>42,43</sup> In this case, the algal species with the highest Pt  
397 body burden, i.e. *P. subcapitata*, would be expected to exhibit most oxidative stress. However, most  
398 oxidative stress was found in *C. reinhardtii* cells. In contrast, *P. subcapitata* was the most affected  
399 species in the growth inhibition tests. Thus, oxidative stress and growth rate inhibition appear  
400 unrelated. Generally, ROS generation and oxidative stress has been suggested as likely mechanisms  
401 related to NP toxicity in algae and other aquatic microorganisms, although the causal link between  
402 particle properties and ROS generation or effects is not yet established.<sup>42</sup> The formation of extra- or  
403 intracellular ROS can trigger a cascade of cellular events that may cause toxicity.<sup>42</sup> The reverse may  
404 also occur, i.e. that NPs induce toxicity by another mechanism, such as DNA lesions, leading to  
405 cellular stress and accumulation of intracellular ROS.<sup>43</sup> DNA damage is a known effect of platinum  
406 compounds and is also confirmed for PtNPs in human cells.<sup>35,36</sup> However, whether DNA damage  
407 results in cytotoxicity strongly depends on the nature of formed DNA adducts, as documented for the  
408 stereoisomers cis- and transplatin in their toxicity towards cancer cells.<sup>35</sup> Least oxidative stress was  
409 found for *P. subcapitata* even though higher toxicity occurred for this species and more abiotic ROS  
410 was produced in the medium of this species (ISO medium). The many pathways interlinking  
411 abiotic/biotic ROS, oxidative stress, DNA damage and cellular toxicity challenge the establishment of  
412 causality.

413 Our results demonstrate that shading is an important artefact in standard algal growth rate inhibition  
414 testing of PtNPs. If not taken into account, the standard method is not applicable for regulatory hazard  
415 identification purposes. The shading issue will be relevant for other NPs as well, especially those with

416 EC<sub>50</sub> values in the higher end of the classification range (10-100 mg/L) and those adhering strongly to  
417 the algal surface. While the environmental relevance of toxicity testing of NPs at such high  
418 concentration levels is questionable, it is of high regulatory relevance for toxicity identification and  
419 ranking as well as classification, and labeling of NPs within the current regulatory framework. The  
420 cellular toxicity quantified by flow cytometry revealed no marked membrane damage, but significant  
421 oxidative stress in both algal species. This may be linked with abiotic ROS generated by the PtNPs. For  
422 *P. subcapitata*, PtNPs caused both growth rate inhibition and oxidative stress in higher levels than what  
423 could be accounted for by dissolved Pt. This indicates a NP-specific effect possibly related to the  
424 catalytic properties of PtNPs and/or their adhesion to algal cells. Overall, *P. subcapitata* was more  
425 sensitive to the effects of PtNPs than *C. reinhardtii*. Furthermore, higher body burdens were measured  
426 for *P. subcapitata*, most likely due to favored binding of Pt to the polysaccharide containing cell wall  
427 of this algal species. The multi-method approach in this study provided insight into the possible  
428 underlying mechanisms behind the observed PtNP-cell interaction and toxicity. Until more knowledge  
429 on NP-specific toxicity mechanisms becomes available, it is crucial to investigate and account for  
430 artefacts and NP interactions with organisms and media. Generally, a broader and more exploratory  
431 approach to aquatic toxicity testing, employing various endpoints and testing methods, may assist to  
432 avoid false negative as well as false positive test results and advance the understanding within the field  
433 of nanoecotoxicology.

## ACKNOWLEDGEMENTS

434

435 The authors thank Signe Qualmann (DTU Environment), Giulia Cheloni, Nadia von Moos, Séverine Le  
436 Faucheur, Coralie Susicillon, Rebecca Flück, Sophie Moisset and Sonia Blanco-Amijeiras (University  
437 of Geneva) for assistance with technical and practical matters. This work is part of the project  
438 ENVNANO (Environmental Effects and Risk Evaluation of Engineered Nanoparticles) supported by  
439 the European Research Council (grant no. 281579). Javier Jiménez-Lamana acknowledges the  
440 European Commission for receiving funding from the European Union's Horizon 2020 research and  
441 innovation program under the Marie Skłodowska-Curie grant agreement No. 660590.

442

## REFERENCES

- 443 (1) Juganson, K.; Ivask, A.; Blinova, I.; Mortimer, M.; and Kahru, A. NanoE-Tox: New and in-depth  
444 database concerning ecotoxicity of nanomaterials. *Beilstein J. Nanotechnol.* **2015**, *6*, 1788–1804.
- 445 (2) Artelt, S.; Creutzenberg, O.; Kock, H.; Levsen, K.; Nachtigall, D.; Heinrich, U.; Rühle, T.; and  
446 Schlögl, R. Bioavailability of fine dispersed platinum as emitted from automotive catalytic converter:  
447 A model study. *Sci. Total Environ.* **1999**, *228*, 217–226.
- 448 (3) Rühle, T.; Schneider, H.; Find, J.; Herein, D.; Pfänder, N.; Wild, U.; Schlogl, R.; Nachtigall, D.;  
449 Artelt, S.; Heinrich, U.; Rühle, T.; Schneider, H.; Find, J.; Herein, D.; Pfänder, N.; Wild, U.; Schlögl,  
450 R.; Nachtigall, D.; Artelt, S.; and Heinrich, U. Preparation and characterisation of Pt/Al<sub>2</sub>O<sub>3</sub> aerosol  
451 precursors as model Pt-emissions from catalytic converters. *Appl. Catal. B-Environmental* **1997**, *14*,  
452 69–84.
- 453 (4) Engelbrekt, C.; Sørensen, K. H.; Lübcke, T.; Zhang, J.; Li, Q.; Pan, C.; Bjerrum, N. J.; and Ulstrup,  
454 J. 1.7 nm Platinum Nanoparticles: Synthesis with Glucose Starch, Characterization and Catalysis.  
455 *Chemphyschem* **2010**, *11*, 2844–2853.
- 456 (5) Merget, R.; and Rosner, G. Evaluation of the health risk of platinum group metals emitted from  
457 automotive catalytic converters. *Sci. Total Environ.* **2001**, *270*, 165–173.
- 458 (6) Reith, F.; Campbell, S. G.; Ball, A. S.; Pring, A.; and Southam, G. Platinum in Earth surface  
459 environments. *Earth-Science Rev.* **2014**, *131*, 1–21.
- 460 (7) Haus, N.; Zimmermann, S.; Wiegand, J.; and Sures, B. Occurrence of platinum and additional  
461 traffic related heavy metals in sediments and biota. *Chemosphere* **2007**, *66*, 619–629.
- 462 (8) Barbante, C.; Veyseyre, A.; Ferrari, C.; Van de Velde, K.; Morel, C.; Capodaglio, G.; Cescon, P.;  
463 Scarponi, G.; and Boutron, C. Greenland snow evidence of large scale atmospheric contamination for  
464 platinum, palladium, and rhodium. *Environ. Sci. Technol.* **2001**, *35*, 835–839.

- 465 (9) Asharani, P. V.; Lianwu, Y.; Gong, Z.; and Valiyaveettil, S. Comparison of the toxicity of silver,  
466 gold and platinum nanoparticles in developing zebrafish embryos. *Nanotoxicology* **2011**, *5*, 43–54.
- 467 (10) George, S.; Xia, T.; Rallo, R.; Zhao, Y.; Ji, Z.; Lin, S.; Wang, X.; Zhang, H.; France, B.;  
468 Schoenfeld, D.; Damoiseaux, R.; Liu, R.; Lin, S.; Bradley, K. A.; Cohen, Y.; and Nel, A. E. Use of a  
469 High-Throughput Screening Approach Coupled with In Vivo Zebrafish Embryo Screening To Develop  
470 Hazard Ranking for Engineered Nanomaterials. *ACS Nano* **2011**, *5*, 1805–1817.
- 471 (11) Ksiazek, M.; Asztemborska, M.; Steborowski, R.; and Bystrzejewska-Piotrowska, G. Toxic Effect  
472 of Silver and Platinum Nanoparticles Toward the Freshwater Microalga *Pseudokirchneriella*  
473 *subcapitata*. *Bull. Environ. Contam. Toxicol.* **2015**, *94*, 554–558.
- 474 (12) European Parliament and Council. Regulation (EC) No 1272/2008 of the European Parliament and  
475 of the Council of 16 December 2008 on classification, labelling and packaging of substances and  
476 mixtures. *Off. J. Eur. Union* **2008**, 353.
- 477 (13) Pettitt, M. E.; and Lead, J. R. Minimum physicochemical characterisation requirements for  
478 nanomaterial regulation. *Environ. Int.* **2013**, *52*, 41–50.
- 479 (14) Hartmann, N. B.; von der Kammer, F.; Hofmann, T.; Baalousha, M.; Ottofuelling, S.; and Baun,  
480 A. Algal testing of titanium dioxide nanoparticles-Testing considerations, inhibitory effects and  
481 modification of cadmium bioavailability. *Toxicology* **2010**, *269*, 190–197.
- 482 (15) Hartmann, N. B.; Engelbrekt, C.; Zhang, J.; Ulstrup, J.; Kusk, K. O.; and Baun, A. The challenges  
483 of testing metal and metal oxide nanoparticles in algal bioassays: titanium dioxide and gold  
484 nanoparticles as case studies. *Nanotoxicology* **2013**, *7*, 1082–1094.
- 485 (16) Sørensen, S. N.; and Baun, A. Controlling silver nanoparticle exposure in algal toxicity testing - A  
486 matter of timing. *Nanotoxicology* **2015**, *9*, 201–209.
- 487 (17) Handy, R. D.; van den Brink, N.; Chappell, M.; Mühlhng, M.; Behra, R.; Dusinska, M.; Simpson,

488 P.; Ahtiainen, J.; Jha, A. N.; Seiter, J.; Bednar, A.; Kennedy, A.; Fernandes, T. F.; and Riediker, M.  
489 Practical considerations for conducting ecotoxicity test methods with manufactured nanomaterials:  
490 What have we learnt so far? *Ecotoxicology* **2012**, *21*, 933–972.

491 (18) Sørensen, S. N.; Hjorth, R.; Delgado, C. G.; Hartmann, N. B.; and Baun, A. Nanoparticle  
492 ecotoxicity-physical and/or chemical effects? *Integr. Environ. Assess. Manag.* **2015**, *11*, 722–724.

493 (19) (OECD), O. for E. C. and D. Guidance document on the aquatic toxicity testing of difficult  
494 substances and mixtures. **2000**,. Paris, France.

495 (20) Baun, A.; Hartmann, N. B.; Grieger, K. D.; and Hansen, S. F. Setting the limits for engineered  
496 nanoparticles in European surface waters - are current approaches appropriate? *J. Environ. Monit.*  
497 **2009**, *11*, 1774–1781.

498 (21) ISO. Water quality - Fresh water algal growth inhibition test with unicellular green algae.  
499 ISO8692:2012. **2012**. International Organization for Standardization, Geneva, Switzerland.

500 (22) Harris, E. H. Chlamydomonas in the laboratory, The Chlamydomonas Sourcebook. Introduction to  
501 Chlamydomonas and its laboratory use, second ed. **2009**,. Academic Press, San Diego, California,  
502 USA.

503 (23) Ivask, A.; Titma, T.; Visnapuu, M.; Vija, H.; Käkinen, A.; Sihtmäe, M.; Pokhrel, S.; Mädler, L.;  
504 Heinlaan, M.; Kisand, V.; Shimmo, R.; and Kahru, A. Toxicity of 11 Metal Oxide Nanoparticles to  
505 Three Mammalian Cell Types In Vitro. *Curr. Top. Med. Chem.* **2015**, *15*, 1914–1929.

506 (24) Arensberg, P.; Hemmingsen, V. H.; and Nyholm, N. A Miniscale Algal Toxicity Test.  
507 *Chemosphere* **1995**, *30*, 2103–2115.

508 (25) Mayer, P.; Cuhel, R.; and Nyholm, N. A simple in vitro fluorescence method for biomass  
509 measurements in algal growth inhibition tests. *Water Res.* **1997**, *31*, 2525–2531.

510 (26) Cheloni, G.; Cosio, C.; and Slaveykova, V. I. Antagonistic and synergistic effects of light

511 irradiation on the effects of copper on *Chlamydomonas reinhardtii*. *Aquat. Toxicol.* **2014**, *155*, 275–  
512 282.

513 (27) von Moos, N.; Maillard, L.; and Slaveykova, V. I. Dynamics of sub-lethal effects of nano-CuO on  
514 the microalga *Chlamydomonas reinhardtii* during short-term exposure. *Aquat. Toxicol.* **2015**, *161*, 267–  
515 275.

516 (28) Christensen, E. R.; Kusk, K. O.; and Nyholm, N. Dose-Response Regressions for Algal Growth  
517 and Similar Continuous Endpoints: Calculation of Effective Concentrations. *Environ. Toxicol. Chem.*  
518 **2009**, *28*, 826–835.

519 (29) Elder, A.; Yang, H.; Gwiazda, R.; Teng, X.; Thurston, S.; He, H.; and Oberdörster, G. Testing  
520 nanomaterials of unknown toxicity: An example based on platinum nanoparticles of different shapes.  
521 *Adv. Mater.* **2007**, *19*, 3124–3129.

522 (30) Hjorth, R.; Sørensen, S. N.; Olsson, M. E.; Baun, A.; and Hartmann, N. B. A certain shade of  
523 green: can algal pigments reveal shading effects of nanoparticles? *Integr. Environ. Assess. Manag.*  
524 **2015**, *12*, 200–202.

525 (31) van Hoecke, K.; De Schampelaere, K. A. C.; Ali, Z.; Zhang, F.; Elsaesser, A.; Rivera-Gil, P.;  
526 Parak, W. J.; Smagghe, G.; Howard, C. V.; and Janssen, C. R. Ecotoxicity and uptake of polymer  
527 coated gold nanoparticles. *Nanotoxicology* **2013**, *7*, 37–47.

528 (32) Schwab, F.; Bucheli, T. D.; Lukhele, L. P.; Magrez, A.; Nowack, B.; Sigg, L.; and Knauer, K. Are  
529 Carbon Nanotube Effects on Green Algae Caused by Shading and Agglomeration? *Environ. Sci.*  
530 *Technol.* **2011**, *45*, 6136–6144.

531 (33) Aruoja, V.; Dubourguier, H. C.; Kasemets, K.; and Kahru, A. Toxicity of nanoparticles of CuO,  
532 ZnO and TiO<sub>2</sub> to microalgae *Pseudokirchneriella subcapitata*. *Sci. Total Environ.* **2009**, *407*, 1461–  
533 1468.

- 534 (34) Clark, A.; Zhu, A.; Sun, K.; and Petty, H. R. Cerium oxide and platinum nanoparticles protect  
535 cells from oxidant-mediated apoptosis. *J. Nanoparticle Res.* **2011**, *13*, 5547–5555.
- 536 (35) Gehrke, H.; Pelka, J.; Hartinger, C. G.; Blank, H.; Bleimund, F.; Schneider, R.; Gerthsen, D.;  
537 Bräse, S.; Crone, M.; Türk, M.; and Marko, D. Platinum nanoparticles and their cellular uptake and  
538 DNA platination at non-cytotoxic concentrations. *Arch. Toxicol.* **2011**, *85*, 799–812.
- 539 (36) Asharani, P. V.; Xinyi, N.; Hande, M. P.; and Valiyaveetil, S. DNA damage and p53-mediated  
540 growth arrest in human cells treated with platinum nanoparticles. *Nanomedicine* **2010**, *5*, 51–64.
- 541 (37) van den Hoek, C.; Mann, D. G.; and Jahns, H. M. Algae: An introduction to phycology. *Algae An*  
542 *Introd. to Phycol.* Cambridge University Press, 40 W. 20th Street, New York, New York 10011-4211,  
543 USA; Cambridge University Press, The Pitt Building, Trumpington Street, Cambridge CB2 1RP,  
544 England.
- 545 (38) Rauch, S.; Paulsson, M.; Wilewska, M.; Blanck, H.; and Morrison, G. M. Short-term toxicity and  
546 binding of platinum to freshwater periphyton communities. *Arch. Environ. Contam. Toxicol.* **2004**, *47*,  
547 290–296.
- 548 (39) Colombo, C.; Oates, C. J.; Monhemius, A. J.; and Plant, J. A. Complexation of platinum,  
549 palladium and rhodium with inorganic ligands in the environment. *Geochemistry Explor. Environ.*  
550 *Anal.* **2008**, *8*, 91–101.
- 551 (40) Šebek, O.; Mihaljevič, M.; Strnad, L.; Ettlér, V.; Ježek, J.; Štědrý, R.; Drahotá, P.; Ackerman, L.;  
552 and Adamec, V. Dissolution kinetics of Pd and Pt from automobile catalysts by naturally occurring  
553 complexing agents. *J. Hazard. Mater.* **2011**, *198*, 331–339.
- 554 (41) Nachtigall, D.; Artelt, S.; and Wunsch, G. Speciation of platinum–chloro complexes and their  
555 hydrolysis products by ion chromatography Determination of platinum oxidation states. *J. Chromatogr.*  
556 **1997**, *775*, 197–210.

557 (42) von Moos, N.; and Slaveykova, V. I. Oxidative stress induced by inorganic nanoparticles in  
558 bacteria and aquatic microalgae - state of the art and knowledge gaps. *Nanotoxicology* **2014**, *8*, 605–  
559 630.

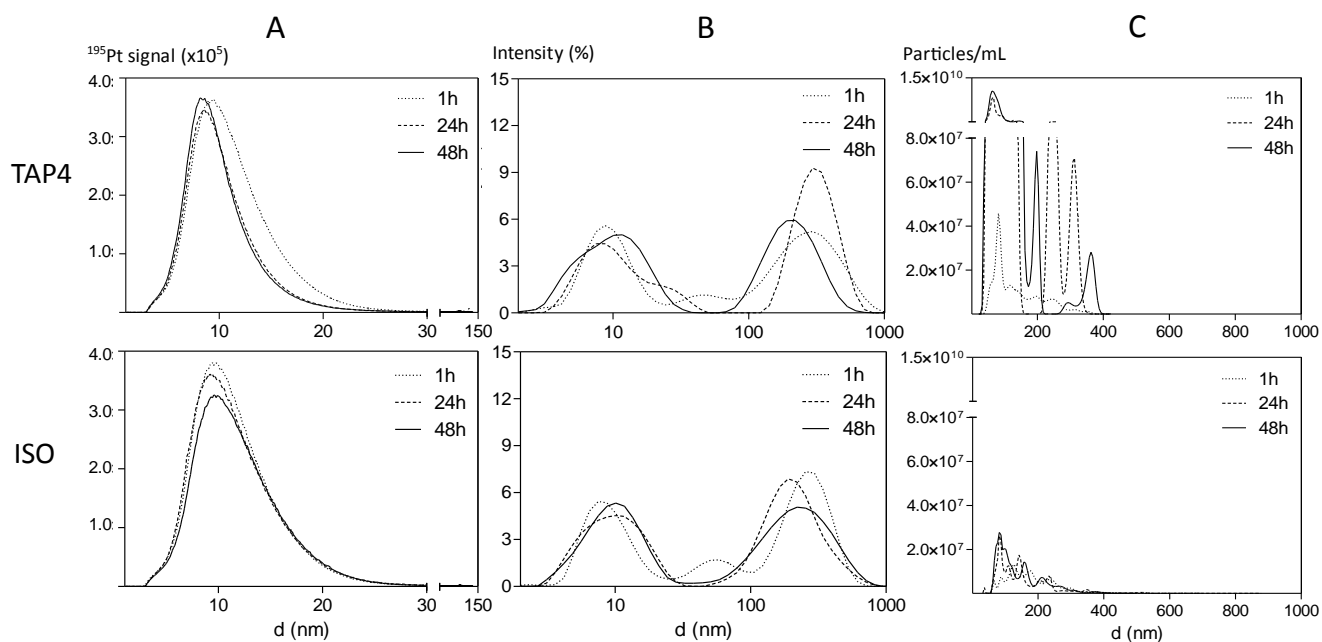
560 (43) Kaweeteerawat, C.; Ivask, A.; Liu, R.; Zhang, H.; Chang, C. H.; Low-Kam, C.; Fischer, H.; Ji, Z.;  
561 Pokhrel, S.; Cohen, Y.; Telesca, D.; Zink, J.; Mädler, L.; Holden, P. A.; Nel, A.; and Godwin, H.  
562 Toxicity of Metal Oxide Nanoparticles in Escherichia coli Correlates with Conduction Band and  
563 Hydration Energies. *Environ. Sci. Technol.* **2015**, *49*, 1105–1112.

564

## SUPPORTING INFORMATION

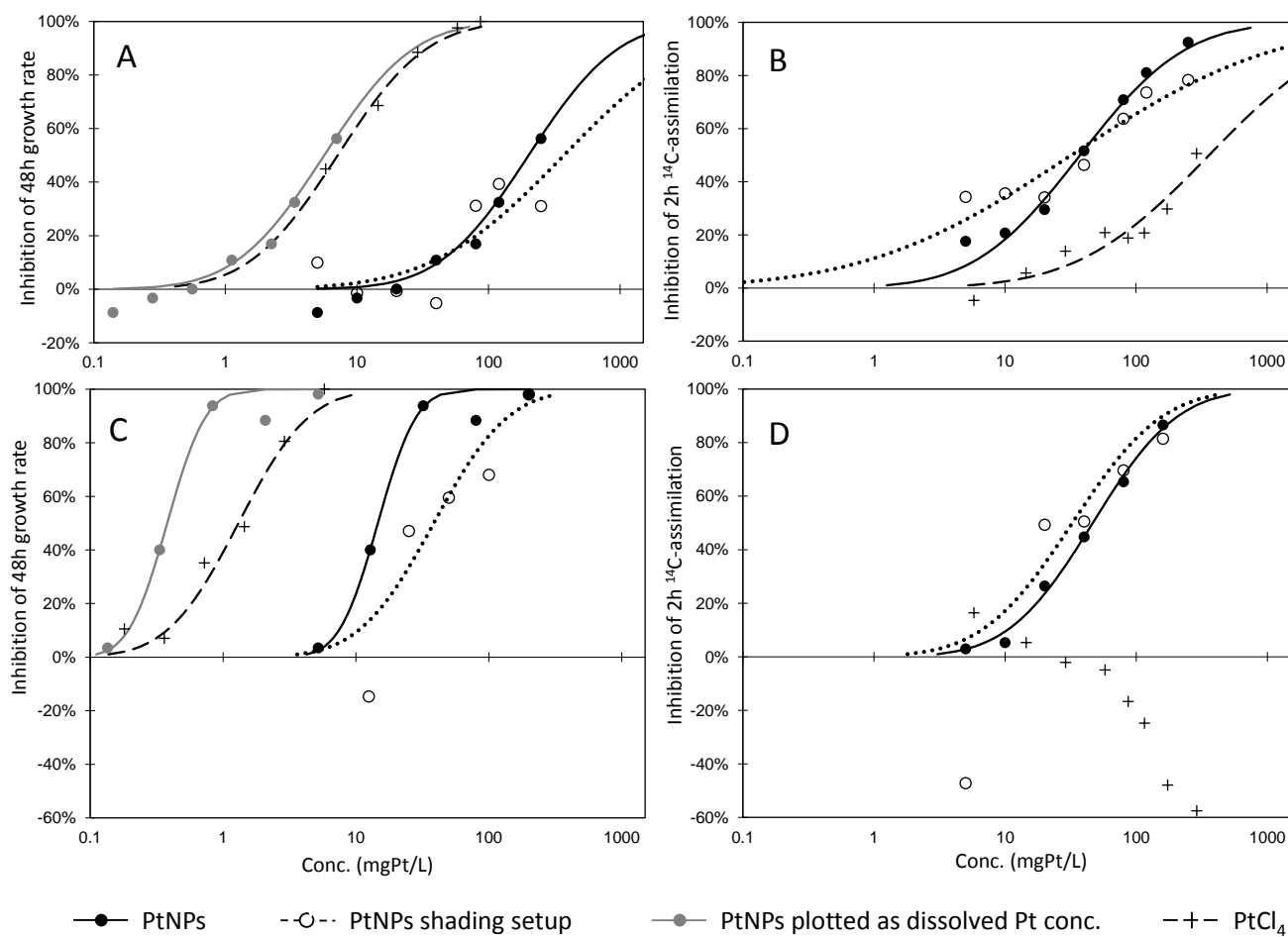
565

566 Additional experimental details regarding size distribution measurements by AsFIFFF, abiotic ROS  
567 formation by PtNPs and PtCl<sub>4</sub>, algal culturing, algal shading and <sup>14</sup>C-assimilation tests, gating  
568 strategies for flow cytometry, as well as determination of the potential photochemical efficiency of  
569 PSII in algae. Results and data for sedimentation of PtNPs in algal media, abiotic ROS generation by  
570 PtNPs and PtCl<sub>4</sub> in algal media, potential PSII photochemical efficiency and membrane damage in  
571 algae, and atomic force microscopy images of algal cells exposed to PtNPs.



572

573 **Figure 1.** Size distributions after different incubation periods (1-48h) for PtNPs suspended in TAP4  
 574 medium (top row) and ISO medium (bottom row) determined by different methods. Column A)  
 575 Suspensions of 4 mg Pt/L analyzed by Asymmetric Flow Field-Flow Fractionation (AsFIFFF); Column  
 576 B) Suspensions of 30 mg Pt/L analyzed by Dynamic Light Scattering (DLS); Column C) Suspensions  
 577 of 80 mg Pt/L analyzed by Nanoparticle Tracking Analysis (NTA).



578

579

580

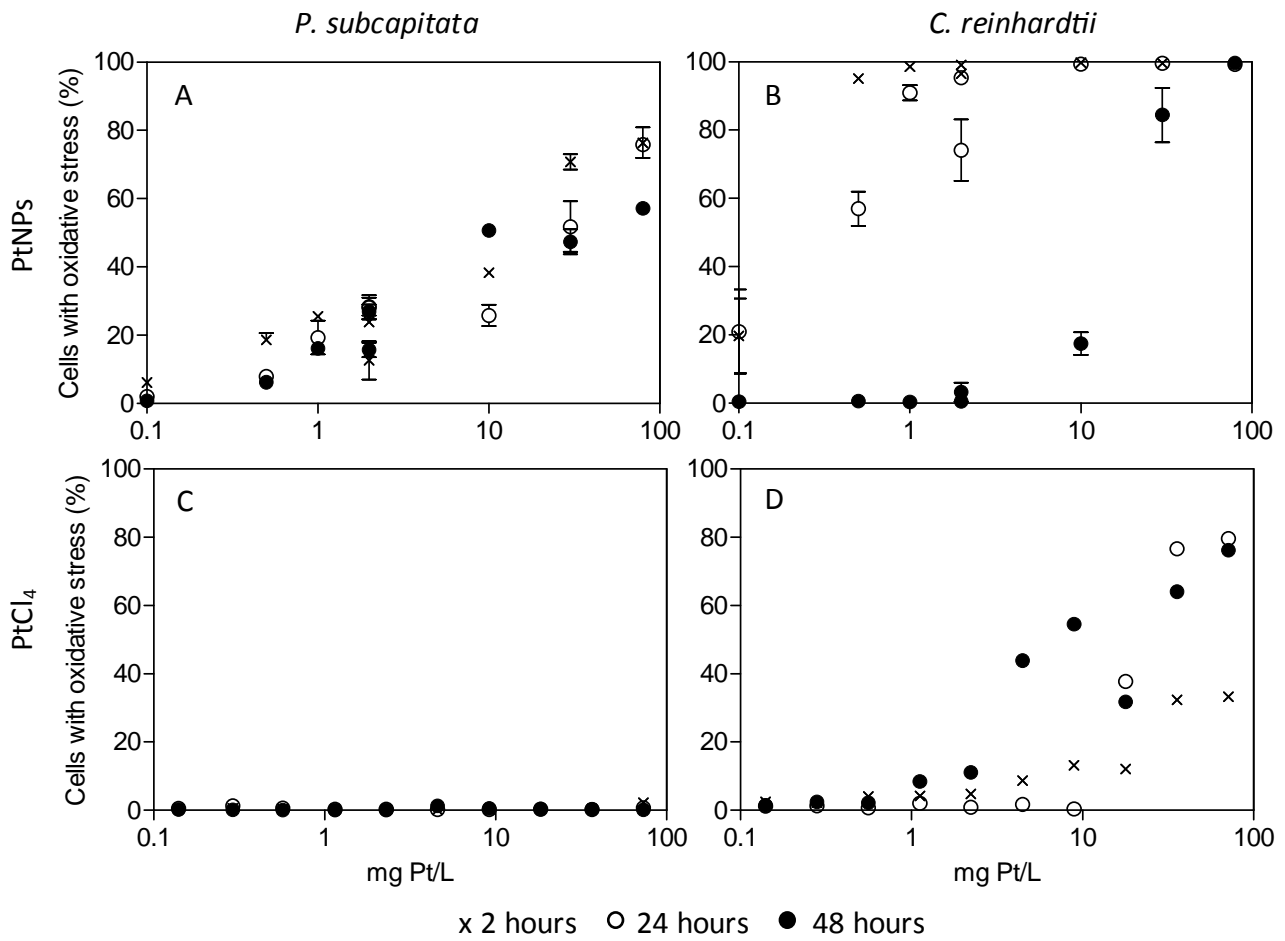
581

582

583

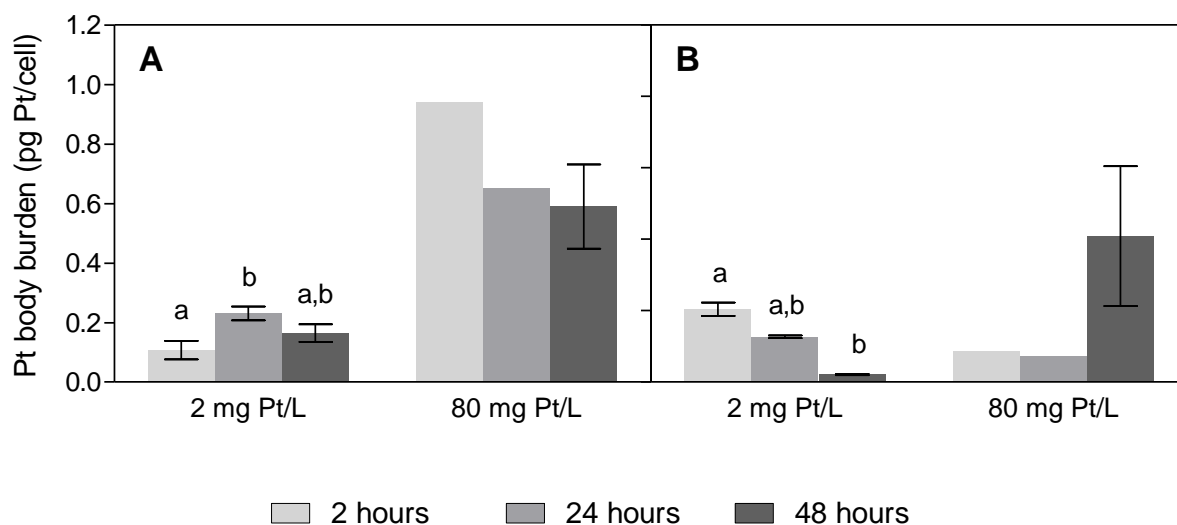
584

**Figure 2.** Concentration-response data and fitted curves from 48 h growth rate inhibition tests (A and C) and 2 h <sup>14</sup>C-assimilation tests (B and D) with *C. reinhardtii* (A and B) and *P. subcapitata* (C and D) for PtNPs and PtCl<sub>4</sub>. For PtNPs two setups were applied in accordance with Figure S1: A regular setup and a double-vial setup for investigation of shading effects. Furthermore, the concentration-response data and curves for PtNPs was recalculated based on the dissolved Pt fraction, and plotted for A and C to reflect the toxicity of the dissolved Pt in the PtNP suspension.



585 x 2 hours ○ 24 hours ● 48 hours

586 **Figure 3.** Oxidative stress in *P. subcapitata* and *C. reinhardtii* upon 2, 24 and 48 h exposure to PtCl<sub>4</sub>,  
 587 in single concentrations (0.14-73 mg Pt/L) and PtNPs in two parallel tests with triplicate low  
 588 concentrations (0.1-2 mg Pt/L) and high (2-80 mg Pt/L), respectively. Data for *C. reinhardtii* exposed  
 589 to PtCl<sub>4</sub> for 2 h are based on very low cells numbers. The error bars represent standard deviations.



590

591 **Figure 4.** Body burdens of platinum for *P. subcapitata* (A) and *C. reinhardtii* (B) after 2, 24 and 48 h  
 592 exposure to PtNPs at 2 and 80 mg Pt/L. The error bars represent standard deviations. For body burdens  
 593 determined at 80 mg Pt/L after 2 and 24 hours n=2 or n=1. For all other data n=3. The letters “a” and  
 594 “b” denotes statistically significant differences in medians ( $p < 0.05$ ) according to Kruskal-Wallis and  
 595 Dunn’s multiple comparison tests, over time within each algal species and exposure concentration  
 596 treatment.

## Supporting information

### A Multimethod Approach for Investigating Algal Toxicity of Platinum Nanoparticles

Sara N. Sørensen<sup>†\*</sup>, Christian Engelbrekt<sup>‡</sup>, Hans-Christian H. Lützhøft<sup>†</sup>, Javier Jiménez-Lamana<sup>§</sup>, Jafar Noori<sup>||</sup>, Fatima A. Alatraktchi<sup>⊥</sup>, Cristina G. Delgado<sup>†</sup>, Vera I. Slaveykova<sup>§</sup> and Anders Baun<sup>†</sup>

#### Corresponding author

Name: Sara Nørgaard Sørensen

Address: Department of Environmental Engineering, Technical University of Denmark  
Miljøvej, Building 113, DK-2800 Kongens Lyngby, Denmark

Phone: +45 45251688 or +45 28556482

Fax: +45 45932850

E-mail: [sans@env.dtu.dk](mailto:sans@env.dtu.dk)

#### This supporting information contains:

16 Pages

2 Tables

9 Figures

20	<b>Table of contents</b>	
21		
22	S1 Materials and methods - additional details including references	Page S3
23	S2 Settings and results for AsFIFFF measurements	Page S7
24	S3 Experimental setup for shading experiments	Page S8
25	S4 Flow cytometry gating strategies	Page S9
26	S5 Sedimentation of PtNPs in algal media	Page S12
27	S6 Abiotic ROS generation by PtNPs and PtC <sub>14</sub> in algal media	Page S13
28	S7 Potential PSII photochemical efficiency in algae	Page S14
29	S8 Membrane damage in algal cells	Page S15
30	S9 Atomic force microscopy images of algal cells	Page S16

## S1 Materials and methods - additional details, including references.

### **Size distribution measured by AsFIFFF**

Suspensions of 4 mg Pt/L were injected in the separation system and characterized immediately upon preparation and after 1, 24 and 48 h. A spacer of 350  $\mu\text{m}$  thickness, a 20  $\mu\text{L}$  loop and a regenerated cellulose (RC) membrane with a cut-off of 1 kDa were used in all the experiments. 0.01% sodium dodecyl sulfate (SDS) in 1 mM  $\text{NH}_4\text{NO}_3$  (Sigma-Aldrich) solution at pH 8 was used as carrier. The optimal separation program found is detailed in Table S1. In order to characterize the sample, the system was first calibrated against polystyrene standards of known size (22, 58 and 97 nm). The following linear relationship between the logarithm of the retention ratio R (defined as elution time corresponding to the void volume divided by the retention time for a given particle) and the logarithm of the diameter (d) in nanometers was experimentally found:

$$\text{Log}(R) = 0.4939 - 0.9539 \times \text{Log}(d); r = 0.9958 \quad (1)$$

Fractograms obtained as a function of time for each sample were converted into size distributions according to equation (1).

### **Abiotic ROS formation**

$\text{H}_2\text{DCF-DA}$  was dissolved in ethanol (1.3 mM) and deacetylated to  $\text{H}_2\text{DCF}$  by letting 1 mL react with 4 mL 0.01 M NaOH for 30 min in the dark. The mixture was added 20 mL sodium phosphate buffer (25 mM, pH 7.4) and the resulting 52  $\mu\text{M}$   $\text{H}_2\text{DCF}$  solution was placed on ice in the dark until use. PtNPs and  $\text{PtCl}_4$  were added to TAP4 and ISO media in the concentration range 0.001-390 mg Pt/L. After 2 h and 48 h incubation in media, under the same conditions as for growth inhibition testing, 100  $\mu\text{L}$  of the PtNP suspensions was each mixed with 100  $\mu\text{L}$   $\text{H}_2\text{DCF}$  solution in the wells of a 96-well black microplate (three replicates of each concentration). After 1 h incubation in the dark, the fluorescence of DCF was

55 measured (readings, n=3) (excitation/emission at 485/527 nm) using a fluorescence plate reader (Biotek  
56 Synergy Mx plate reader). As positive control, H<sub>2</sub>O<sub>2</sub> was diluted in ISO and TAP4 media in the  
57 concentration range 0.16–20% (w/w). The ROS level in samples was calculated in relative fluorescence  
58 units (RFUs) by dividing the fluorescence of samples (PtNPs in media incubated with H<sub>2</sub>DCF) by  
59 fluorescence of background (media incubated with H<sub>2</sub>DCF).

60

### 61 **Algal culturing**

62 *P. subcapitata* was obtained from the Norwegian Institute for Water Research, Oslo, Norway (NIVA) and  
63 cultivated in ISO 8692 medium<sup>1</sup> and the *C. reinhardtii* strain CPC11 was obtained from the Canadian  
64 Phycological Culture Center (CPCC, Department of Biology, University of Waterloo, Canada) and grown  
65 in four times diluted Tris-Acetate-Phosphate medium<sup>2</sup>. The two respective media are hereafter referred to  
66 as ISO and TAP4 media. For all toxicity testing, the algae were exposed in their respective cultivation  
67 medium and testing was conducted under the same incubation conditions as for the culture. For cellular  
68 toxicity, photosynthesis efficiency and body burden studies 250 mL Erlenmeyer flasks were fitted with  
69 permeable stoppers, containing 50 mL algal suspension and incubated (Infors, Bottmingen, Switzerland)  
70 at 20 ± 2°C with continuous agitation (100 rpm) and illumination from above (110 ± 10 μmol/m<sup>2</sup>/s). For  
71 growth and carbon assimilation inhibition tests 20 mL glass vials with perforated screw cap lids,  
72 containing 5 mL suspension were kept at 20 ± 2°C, continuous shaking (300 rpm) and illuminated from  
73 below by fluorescent tubes (30W/33; Philips, The Netherlands) at a light intensity of 100 ± 20 μmol/m<sup>2</sup>/s.  
74 The algal cultures were re-inoculated in fresh media every second to third day, to ensure an exponentially  
75 growing culture.

76

### 77 **Algal <sup>14</sup>C-assimilation tests**

78 Preparation of test concentrations, control and replicates was similar to the growth rate inhibition tests, but  
79 the initial algal density was  $10^5$  cells/mL. Immediately before incubation, 50  $\mu$ L of  $\text{NaH}^{14}\text{CO}_3$  solution  
80 (specific activity: 20  $\mu\text{Ci/mL}$ ; obtained from DHI, Hoersholm, Denmark) was added to all vials which  
81 were then closed with airtight screw caps. The tests were terminated after 2 h incubation by adding 0.2 mL  
82 10% HCl to each vial (yielding  $\text{pH} < 2$ ). The vials were left open overnight in a fume hood and 10 mL  
83 scintillation liquid (Optiphase “Hisafe” 3, Perkin Elmer, Waltham, MA, USA) was added to each vial.  
84 After thorough mixing, they were left in the dark for 8 h and submitted to liquid scintillation counting  
85 (Hidex 300 SL).  $\text{H}^{14}\text{CO}_3$  solution was also added to three replicates of medium only, as controls to  
86 confirm that all added  $^{14}\text{C}$  that had not incorporated into biomass, was being converted into  $^{14}\text{CO}_2$  and  
87 removed in the evaporation step.

88

### 89 **Potential photochemical efficiency of PSII**

90 Algae exposed to PtNPs at 2 and 80 mg Pt/L, along with a control, were incubated for 48 h in triplicate  
91 100 mL flasks of 25 mL suspension. After 2, 24 and 48 h incubation, samples of 3.5 mL were drawn from  
92 all replicates, and upon 1 h of dark acclimation, fluorescence variables were measured by Fast Repetition  
93 Rate Fluorometry (FRRF) using a FastOcean FRR plus FastAct fluorometer (Chelsea Technologies Group  
94 Ltd). Six acquisitions were run per sample and each acquisition comprised of 36 sequence repeats with  
95 saturation/relaxation phases of 100/40 flashlets per sequence and a 2/50  $\mu\text{s}$  pitch. By use of the program  
96 FastPro8 © (Version 1.0.50, Kevin Oxborough, Chelsea Technologies Group Ltd), the potential  
97 photochemical efficiency of PSII ( $F_v/F_m$ ) was obtained, reflective of changes in the photochemical  
98 energy conversion efficiency.<sup>3</sup> Specific blank corrections with pure medium and PtNPs suspension of 80  
99 mg Pt/L in medium were carried out to rule out a possible direct increase of the fluorescence signal due to  
100 the presence of PtNPs. Fluorescence blank readings were lower than 10% of the sample fluorescence  
101 (22% for 2 h measurements).

102

103 **References**

104 (1) ISO. *Water quality - Fresh water algal growth inhibition test with unicellular green algae.*

105 ISO8692:2012; International Organization for Standardization: Geneva, Switzerland, 2012.

106 (2) Harris, E. H. Chlamydomonas in the laboratory. *The Chlamydomonas Sourcebook. Introduction to*

107 *Chlamydomonas and its laboratory use*, 2nd ed.; Academic Press, San Diego, California, USA, 2009.

108 (3) Greene, R. M.; Kolber, Z. S.; Swift, D. G.; Tindale, N. W.; and Falkowski, P. G. Physiological

109 Limitation of Phytoplankton Photosynthesis in the Eastern Equatorial Pacific Determined from Variability

110 in the Quantum Yield of Fluorescence. *Limnol. Oceanogr.* **1994**, *39*, 1061–1074.

111

## S2 Settings and results for AsFIFFF measurements

112

113

114 **Table S1.** Separation program used for AsFIFFF measurements with an outflow of 1.0 mL/min.

	Time [s]		Crossflow [mL/min]
Injection/focusing	300	Injection flow 0.2 mL/min	2
Crossflow	1200	constant	1
	300	linear decay	0
	300	constant	0

115

116

117 **Table S2.** Diameters and widths of the different size distributions and Pt recoveries obtained by AsFIFFF.

Time for PtNPs in media (h)	ISO 8692 medium			TAP4 medium		
	Size (nm)	Width (nm)	Recovery (%)	Size (nm)	Width (nm)	Recovery (%)
0	9.5	7.2	78 ± 4	9.5	7.1	80 ± 4
1	9.4	7.1	82 ± 4	9.5	6.9	80 ± 4
5	9.5	7.1	87 ± 4	8.4	6.1	75 ± 4
24	9.2	7.4	83 ± 4	8.6	5.4	62 ± 3
48	9.6	7.6	77 ± 4	8.2	5.1	63 ± 3

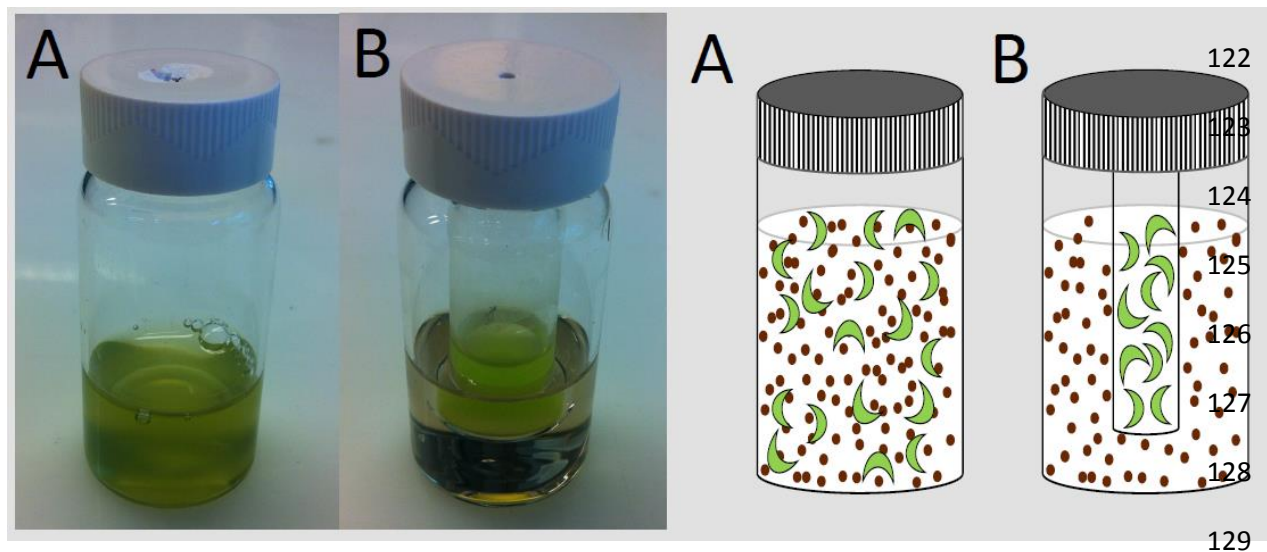
118

### S3 Experimental setup for shading experiments

119

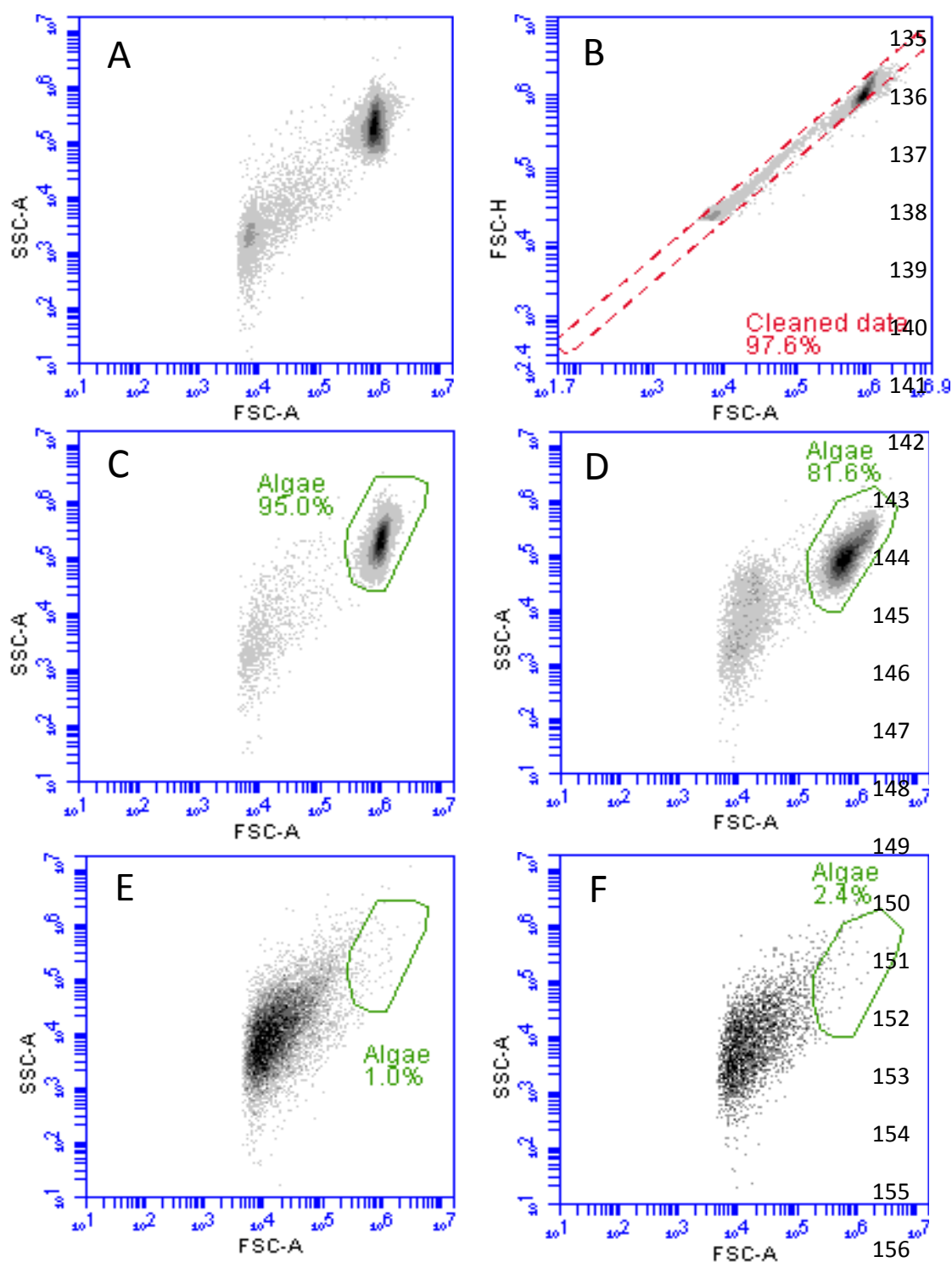
120

121

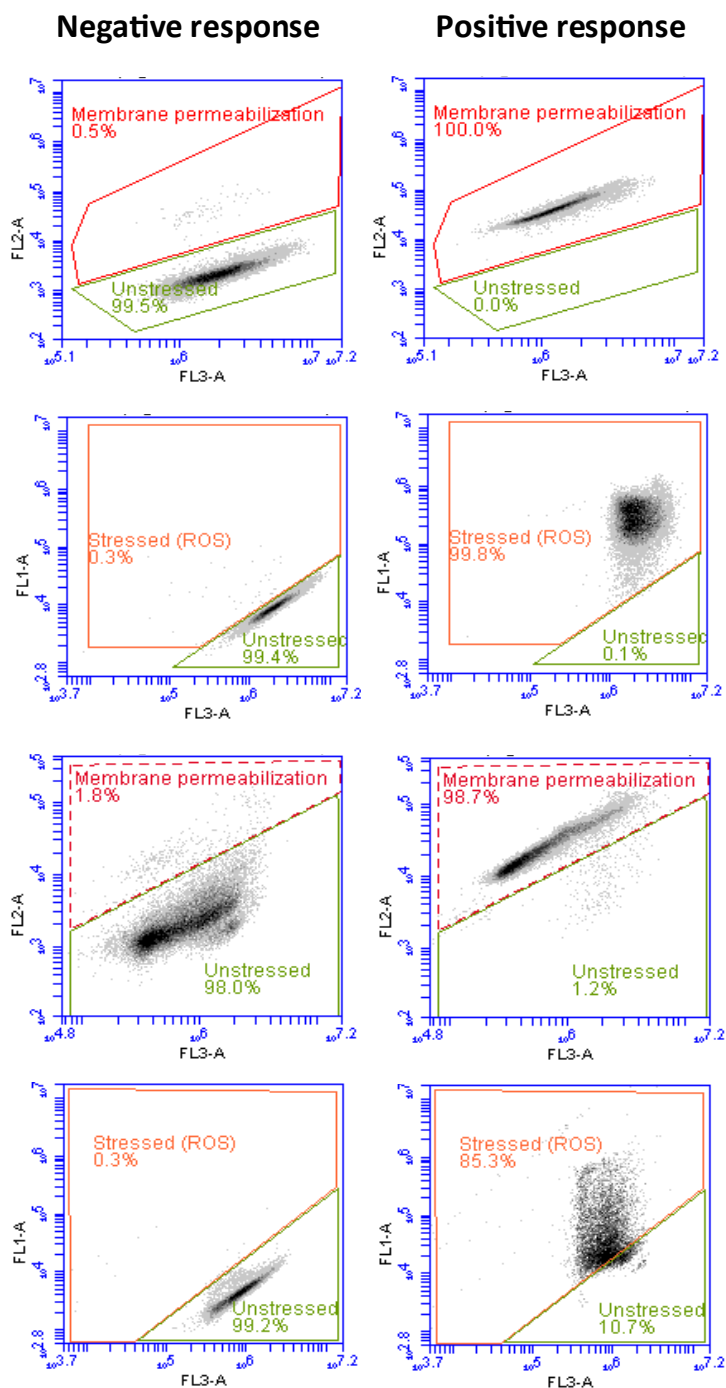


130 **Figure S1.** Photos and illustrations of the test setup used for determining shading effects in the algal  
131 growth inhibition and  $^{14}\text{C}$ -assimilation tests. A) The setup used for standard testing and B) The double-  
132 vial setup, allowing for separation of algal cells in the smaller inner-vial from the surrounding PtNP  
133 suspension in the larger outer-vial.

## S4 Flow cytometry gating strategies

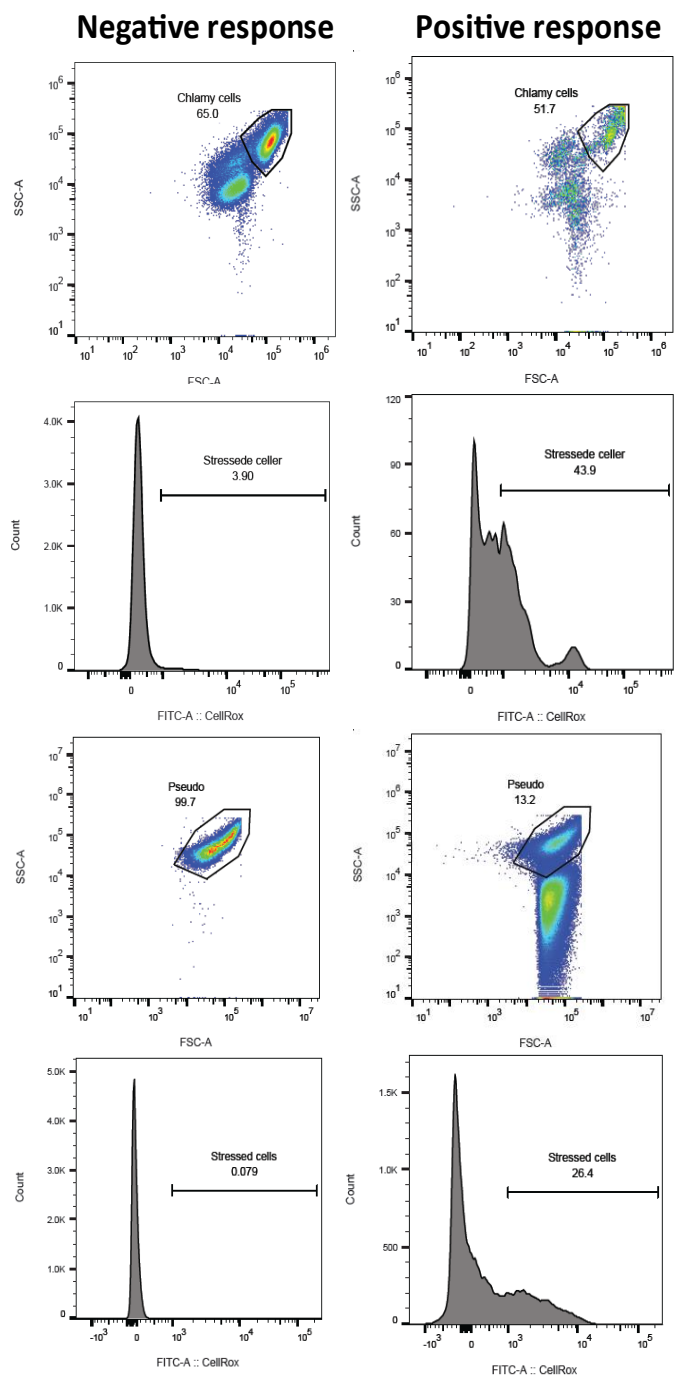


157 **Figure S2.** Flow cytometry gating strategy. A) Raw data for *C. reinhardtii* upon 48 h exposure to PtNPs  
 158 (80 mg PtL), B) Removing doublets with "cleaned data" gate, C) Algal gate for unexposed *C. reinhardtii*,  
 159 D) Algal gate for unexposed *P. subcapitata*, E) PtNPs in TAP4 medium, and F) PtNPs in ISO medium.  
 160 FSC = Forward scatter, SSC = Side scatter, A = Area, H = Height.



161

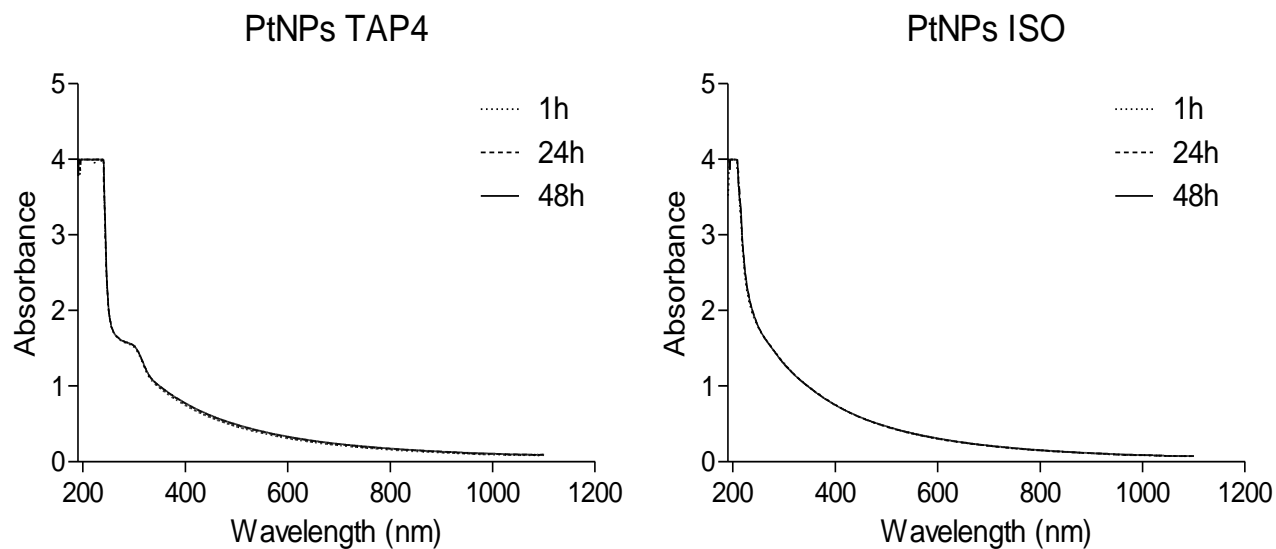
162 **Figure S3.** Flow cytometry gating strategy for biological end points using flow cytometer BD Accuri C6.  
 163 The four graphs on top apply to *C. reinhardtii* and the four below, to *P. subcapitata*. The autofluorescence  
 164 is measured in the fluorescence channel 3 (FL3), membrane permeabilization with the fluorescent probe  
 165 propidium iodide in fluorescence channel 2 (FL2) and oxidative stress with the fluorescent probe  
 166 CellROX green in fluorescence channel 1 (FL1). The gates are determined based on the negative and  
 167 positive controls, except for CellROX in *P. subcapitata*, as H<sub>2</sub>O<sub>2</sub> was not a usable positive control for this  
 168 alga/medium. The experiments are considered valid, as a very clear response was obtained from algae  
 169 exposed to PtNPs.



170

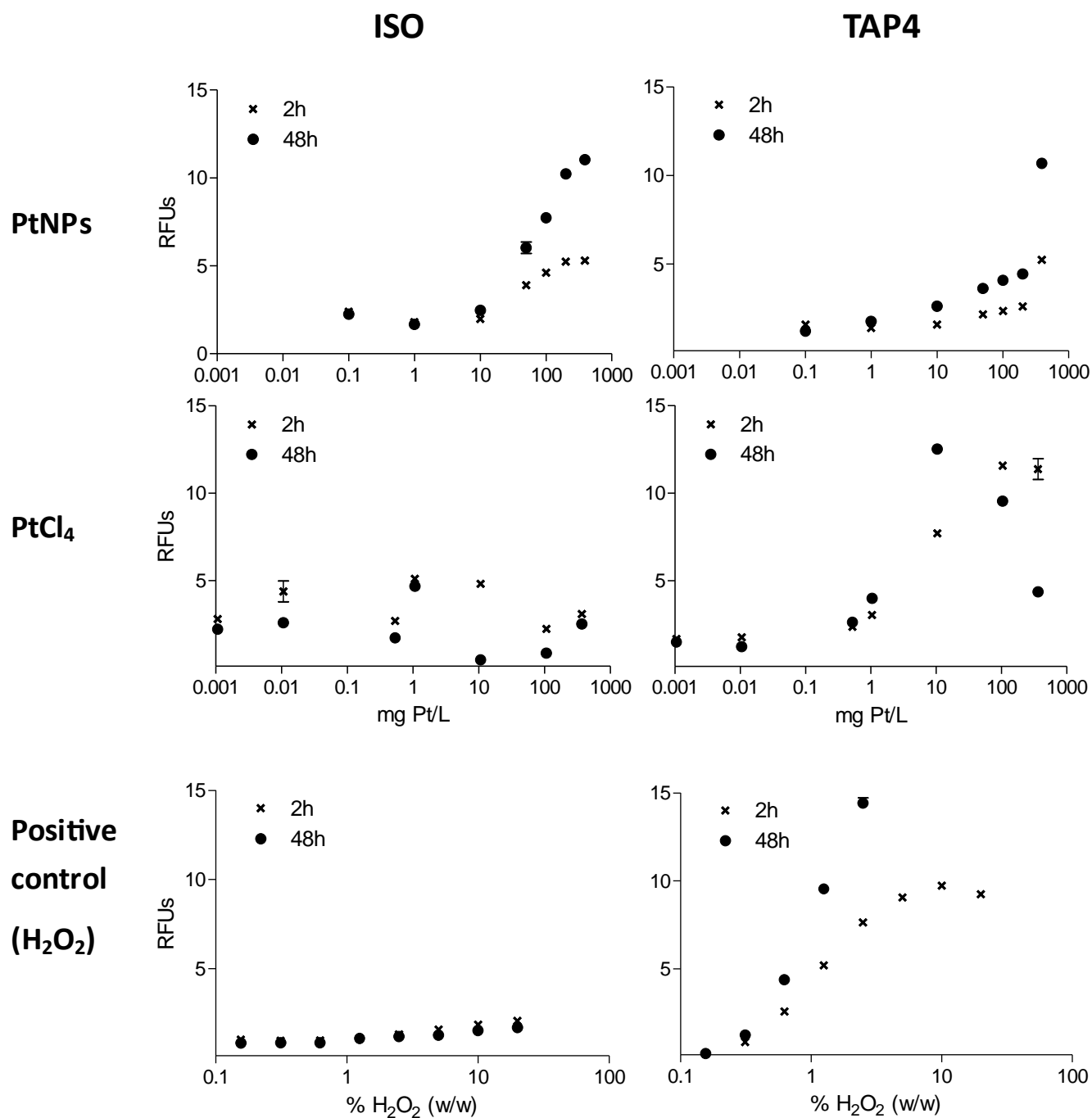
171 **Figure S4.** Flow cytometry gating strategy for biological end points using flow cytometer BD  
 172 FACSCanto II. The four top graphs apply to *C. reinhardtii* and the four below, to *P. subcapitata*. The  
 173 oxidative stress response is determined by the fluorescence of CellROX green in the FITC channel 1 of  
 174 algal cells in the assigned gates. For *C. reinhardtii* a likely contamination was observed, and algal cells  
 175 were distinguished by autofluorescence of algal pigments at 690 nm. The gates are determined based on  
 176 negative and positive controls, except for CellROX in *P. subcapitata*, as H<sub>2</sub>O<sub>2</sub> was not a usable positive  
 177 control for this alga/medium. The experiments are considered valid, as a very clear response was obtained  
 178 from algae exposed to PtNPs.

## S5 Sedimentation of PtNPs in algal media



180

181 **Figure S5.** Absorbance spectra for PtNPs (80 mg Pt/L) suspended in ISO and TAP4 algal media after 1,  
182 24, and 48 h.

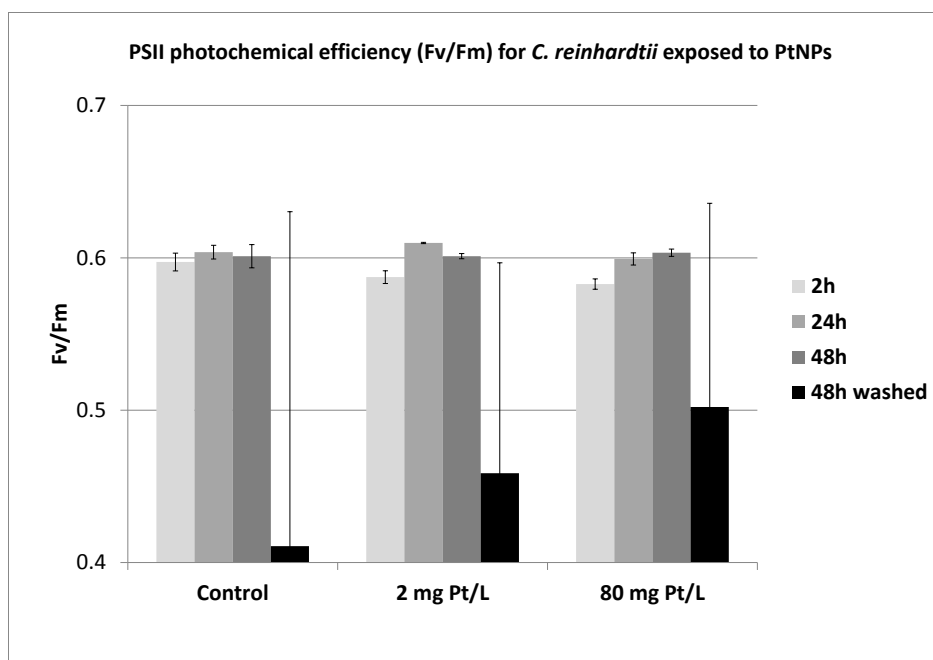
S6 Abiotic ROS generation by PtNPs and PtCl<sub>4</sub> in algal media

184

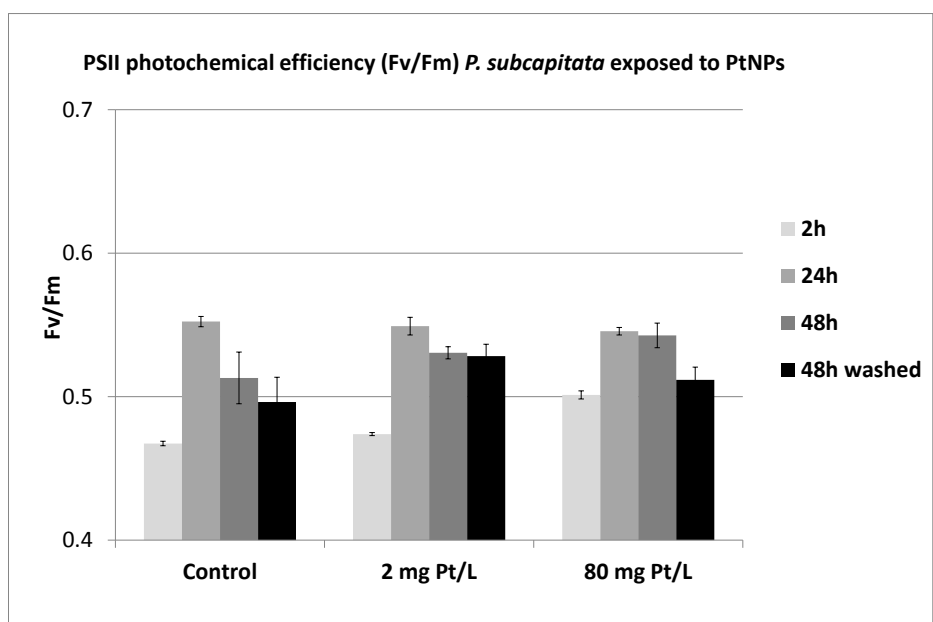
185 **Figure S6.** Abiotic ROS generation of PtNPs, PtCl<sub>4</sub> and the positive control (H<sub>2</sub>O<sub>2</sub>) upon 2 and 48 h  
 186 suspension in ISO and TAP4 algal media, given as relative fluorescence units (RFUs) determined by the  
 187 fluorescence of DCF from the tested suspension, relative to the fluorescence of the background (DCF in  
 188 the respective media). The error bars represent standard deviations (n=3). The fluorescence exceeded the  
 189 detection range in the positive controls of 5-20% w/w H<sub>2</sub>O<sub>2</sub> in TAP4 medium for 48 h measurements.

190

## S7 Potential PSII photochemical efficiency in algae



191

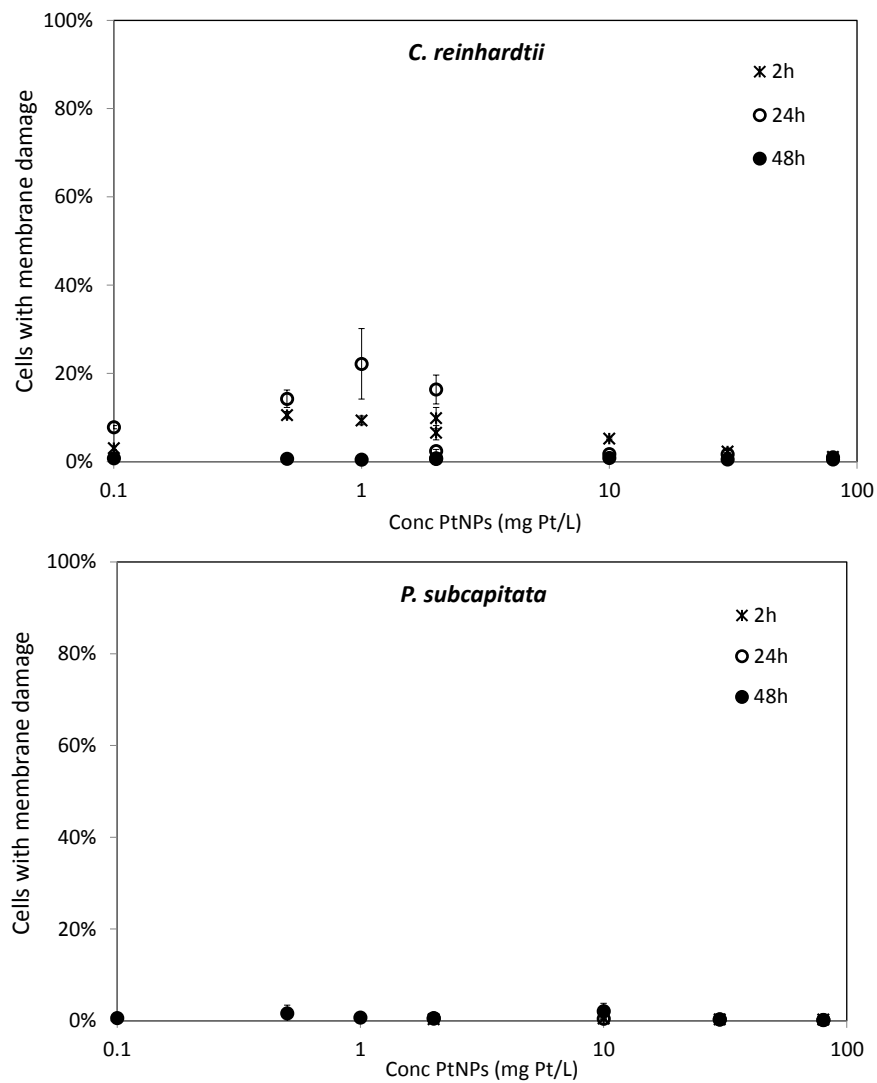


192

193

194 **Figure S7.** Fast Repetition Rate Fluorometry (FRRF) measurements of the potential PSII photochemical  
195 efficiency (Fv/Fm) for *C. reinhardtii* and *P. subcapitata* upon 2, 24 and 48 h exposure to 0, 2 or 80 mg  
196 Pt/L. Measurements were conducted for the algae in the PtNP suspensions, and for 48 h measurements  
197 also for algal cells washed with medium through a filter (48 h washed). The error bars represent standard  
198 deviations (n=3).

## S8 Membrane damage in algal cells

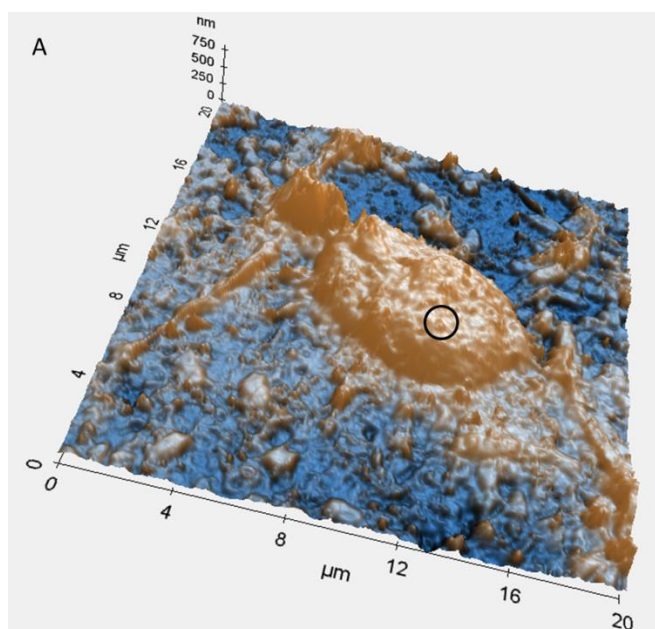


200

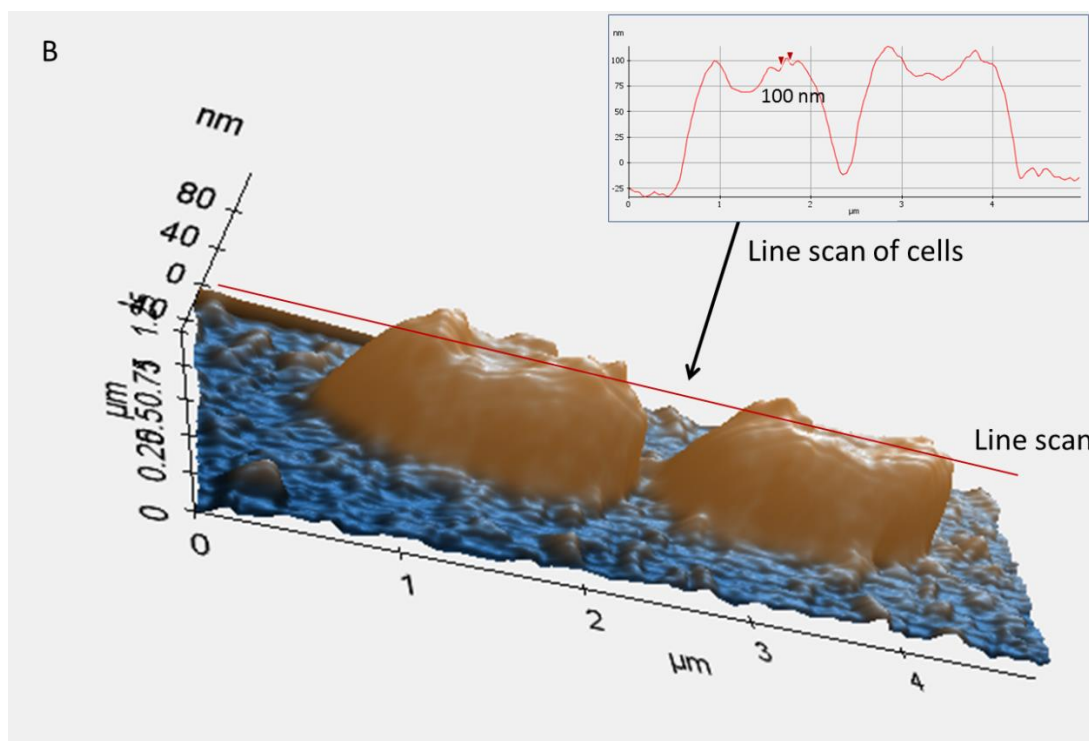
201 **Figure S8.** Membrane damage in *C. reinhardtii* and *P. subcapitata* upon 2, 24 and 48 h exposure to PtNPs  
 202 in two parallel tests with low concentrations (0.1; 0.5; 1 and 2 mg Pt/L nominal) and high concentrations  
 203 (2, 10, 30 and 80 mg Pt/L), respectively. The error bars represent standard deviations (n=3).

204

## S9 Atomic force microscopy images of algal cells



205



206

207 **Figure S9.** AFM visualizations of algal cells after 48 h incubation with PtNPs showing a single cell of *C.*  
208 *reinhardtii* (A) and two cells of *P. subcapitata* (B). The circle shown on the image of *C. reinhardtii* (A)  
209 shows the likely presence of PtNP agglomerates. According to the line scan completed for *P. subcapitata*  
210 (B), structures of app. 100 nm are identified on the cell surface, which may likely be PtNPs agglomerates.